Developments in the Built Environment 13 (2023) 100119

Contents lists available at ScienceDirect

Developments in the Built Environment

journal homepage: www.sciencedirect.com/journal/developments-in-the-built-environment

Masonry patterns' influence on the damage assessment of URM walls: Current and future trends

Simon Szabó [a,*], Marco Francesco Funari [b,**], Paulo B. Lourenço [a]

[a] Department of Civil Engineering, University of Minho, Institute for Sustainability and Innovation in Structural Engineering, Guimarães, 4800 - 058, Portugal
[b] School of Sustainability, Civil and Environmental Engineering, University of Surrey, Guildford, GU2 7XH, United Kingdom

ARTICLE INFO

Keywords:
Historic masonry
Seismic vulnerability
Masonry textures survey
Masonry textures generation

ABSTRACT

While the influence of the component strength on the structural behaviour of Historic Masonry Structures (HMS) is relatively well studied, few studies have investigated masonry textures. Such a research gap is due to the actual difficulty of finding parameters that correlate masonry patterns and structural performances. This paper presents a comprehensive review of the existing geometric measures for irregular masonry patterns, highlighting the gaps and possible future trends. Special attention is paid to the Non-destructive Tests (NDT) for surveying masonry textures and algorithms to generate block-based numerical models artificially. Finally, a numerical investigation underlines how masonry textures generated considering quality indexes present more consistent results.

1. Introduction

Historic masonry structures populate European historic centres as both secular and sacred monumental buildings. Given the (i) important economic and societal role, (ii) high level of material degradation due to time, and (iii) low structural performance under seismic actions, preventive conservation and maintenance of HMS continue to stand as major priorities of the overall political strategy at the European level.

Due to (i) geographical location, (ii) raw material availability, (iii) facilities and (iv) workers' skills, a great variety of building construction techniques for HMS have been developed over the centuries. In this framework, established practices are categorised as reflecting the so-called "rules of art" (*regola d'arte*) (Giuffré, 1996). In Europe, bricks or stones were usually adopted to generate various assemblages, varying bond pattern, number of leaves etc. Referring to brickworks, although there were a large variety of different-sized bricks manufactured, generally, they were rectangular, same-size and arranged in periodic or quasi-periodic patterns (Fig. 1).

On the contrary, making regular arrangements with stone units significantly increased the complexity of the building process, affecting both economic costs and time. For this reason, ancient masons were concerned about generating good-quality masonry patterns by allocating stone units of different sizes and shapes within the wall (Fig. 2). This skill is also reflected in the overall structural performance (Taborda and Roten, 2015).

One should note how the intrinsic properties of HMS, such as high density, low tensile and relatively low shear strength and ductility, lead to their high seismic vulnerability (Lourenço et al., 2017). However, an additional important parameter is the connection degree between structural elements. If the structural elements are (i) properly connected, (ii) the masonry arrangement presents a good quality both in-plane (IP) and through-the-thickness, and (iii) the floors are rigid in their plane, a box-like behaviour of the structure is expected. Consequently, walls will be stressed in their IP direction involving much more ductile collapse (Vlachakis et al., 2020), i.e. progressive generation of cracks precedes the failure. On the contrary, out-of-plane (OOP) failure is much more sudden and destructive (Stepinac and Gašparović, 2020; Stepinac et al., 2020; Lulić et al., 2021). Disintegration and localised failure mechanisms could happen when masonry quality is particularly poor, e.g. masonry is constituted by multiple leaves that are not adequately connected through the thickness (Fig. 3).

It is worth underlining how leaves' connection has a significant effect on the masonry's OOP behaviour (Fig. 4a) (Binda et al., 2006), while the surface pattern primarily affects the structure's IP behaviour and the participation of transversal walls on the OOP response of facades (Fig. 4b) (de Felice et al., 2022a).

One of the main difficulties in studying such a topic is the scarce surveyability of masonry texture cross-sections. Furthermore, even the walls' surfaces are sometimes covered by plaster, and in particular,

* Corresponding author.
** Corresponding author.
E-mail addresses: b12781@civil.uminho.pt (S. Szabó), m.funari@surrey.ac.uk (M.F. Funari).

https://doi.org/10.1016/j.dibe.2023.100119
Received 22 November 2022; Received in revised form 2 January 2023; Accepted 4 January 2023
Available online 9 January 2023

referring to built cultural heritage, only a small part of the surface can be uncovered. Furthermore, even though advanced segmentation algorithms are available in the literature, only the IP pattern can usually be detected, and the transition from discrete or raster data to structural analysis software still needs to be fully automatised (Sithole, 2008; Valero et al., 2018). On the other hand, the knowledge concerning through-the-thickness stones' distribution also poses significant uncertainties, which suggest investigations based on probabilistic approaches rather than deterministic ones, i.e. assuming texture properties within certain statistical variations.

2. Review on masonry arrangements

Across the centuries, various masonry typologies have been used depending on the available stone stocks, facilities and skills of the workers (Binda et al., 1994). Although several factors influenced the masonry patterns, ancient builders consciously tended toward the regular bond pattern with the same-sized units (also called *opus quadratum*) (Giuffré, 1996). This tendency formed the foundations of the so-called "rules of art". The recommendations of the "rules of art" are listed as follows (Caterina, 2001; Baggio and Carocci, 2000).

I Condition for transversal monolithism

Creation of the masonry pattern through the thickness of the wall using stones arranged with their longest length transversal to the wall, often called *diatons*. Larger stones rather than small ones allow IP and through the thickness interlocking. This implies that a vertical joint or unorganised inner core separating the outer leaves must be avoided. The connection of different leaves ensures the transversal monolithic behaviour of the wall.

II Condition for good stone interlocking in a leaf

Mortar must be placed on each stone's face; minimum thickness must be adopted in order to get enough bond. Filling the holes between the large and small stones or bricks is recommended. If such a rule is pursued, the mortar strength will play a secondary role compared to the positive effect of the interlocking of stones.

III Condition for good vertical load transmission

Levelling of bed joints of the masonry at every 0.60–1.00 m along the height of the wall is recommended. The holes between the bigger stones can be filled with smaller stones or bricks; thus, the next course of stones can be placed on a horizontal surface. The presence of horizontal laying surfaces ensures good vertical force transmission.

These three rules are derived from experience accumulated across the centuries; however, their mechanical meaning is intuitive (Giuffré, 1996).

In order to practically assess the quality of the masonry patterns, structural engineers should quantify the patterns deviation with respect to the ideal conditions. This deviation can be assessed by defining a collection of quantitative quality indexes (QI), and their correlation with structural performance.

The following discretisation in subsections is presented. Section 2.1 defines different masonry typologies based on qualitative criteria to determine the deviations between different masonry types. Section 2.2 involves the collection of possible QI-s for the definition of masonry patterns that have high significance on the HMS's structural behaviour. The influence of the masonry pattern on the structural behaviour of HMS is discussed in Section 2.3. Section 2.4 presents typical techniques for the masonry pattern survey, highlighting their advantages and limitations. Finally, masonry pattern generation algorithms are presented in Section 2.5, which can be used to parametrically generate and subsequently assess the effect of masonry pattern quality.

2.1. Masonry typologies

Masonry as a structural material was already used about 8000 years ago (Como, 2016). Most of the ancient civilisations (Egyptians, Romans, Greeks, etc.) used artificial (baked or unbaked bricks) or natural (stones) building blocks bonded together with mud, gypsum, bitumen, lime or cement-based binders to build masonry structures (Taly, 2010). Masonry is still used nowadays, keeping the same driving principles, even though preparation and fabrication procedures are reflecting the digital transformation era (Davis et al., 2012; Rippmann et al., 2016; Ramage H et al., 2021; Deuss et al., 2014). However, the co-presence of different masonry typologies makes the systematic assessment of HMS complex. In order to conduct a detailed categorisation of the masonry typologies, a fundamental prerequisite is the nomenclature knowledge of their component. (Fig. 5).

A general taxonomy might be based on the nature of the units, thus defining groups of stone, brick, adobe and rubble masonry (Carbonara, 1996; Giuffrè, 1990). Further classifications can involve surface texture, cross-section morphology, and the structure's state. Fig. 6a sets the specifications of the rules of art as the origin; thus, the quality of any masonry pattern can be assessed by measuring the deviations from the origin (Fig. 6b). It is worth noting that not all combinations of the above-mentioned parameters exist in real HMS. For example, masonries with heavily worked, squared stones have good morphological properties. Thus, observing real HMS and defining the realistic combinations of values is highly significant. In this framework, extensive surveys on masonry patterns of HMS have been conducted in Italy, resulting in

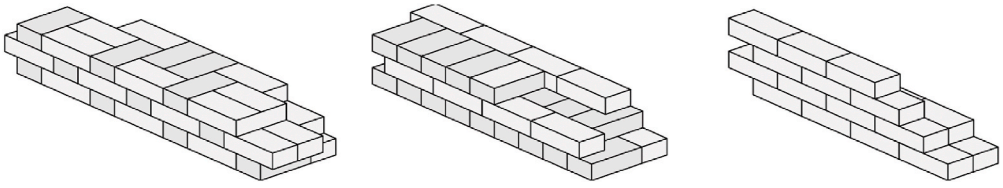

Fig. 1. Different brick masonry arrangements (Como, 2016).

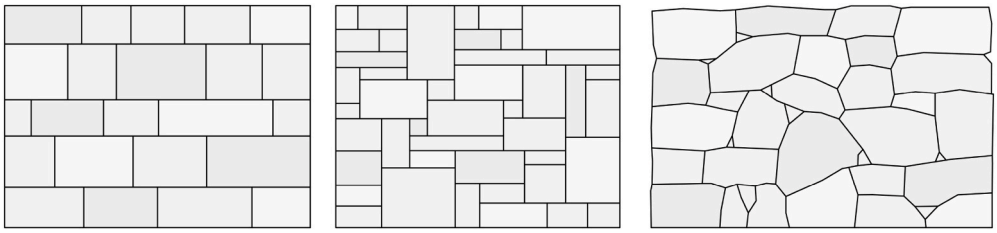

Fig. 2. Different types of stone masonry textures (Taborda and Roten, 2015).

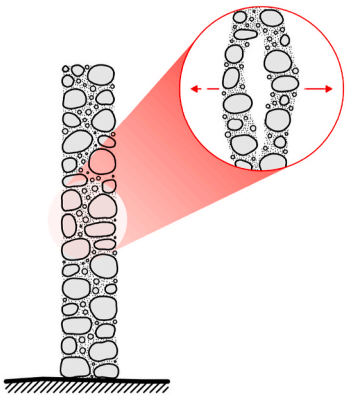

Fig. 3. Disintegration of multi-leaf rubble masonry walls due to lack of transversal connections (Vlachakis et al., 2020).

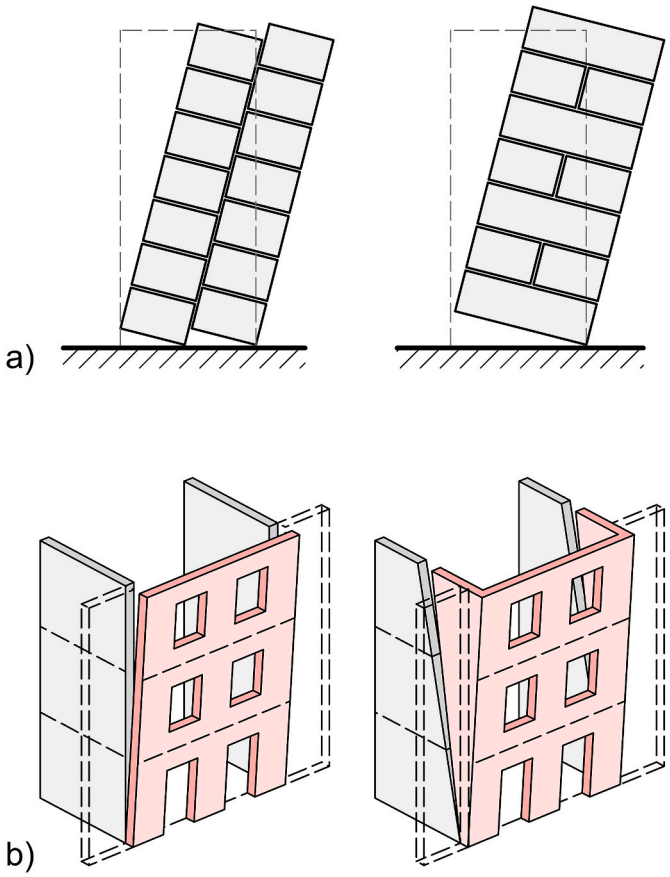

Fig. 4. a) Effect of diatons (Giuffré, 1996) b) Effect of IP pattern (Casapulla et al., 2021) on the OOP failure mechanism.

hundreds of surveyed surfaces and cross-section patterns from different regions (Baggio and Carocci, 2000; Binda et al., 1999). Similar research works have also been conducted in other countries (Ferreira Pinto et al., 2021; Rezaie et al., 2020).

When masonry walls are without plaster, the IP surface is easily detectable, and codes and standards (B. Indian Standards, 1992; CSA Standard S304.1-94, 1994; Bosiljkov et al., 2015; Swiss Society of Engineers and Architects SIA, 2003; GNDT/SNN, 2002; IMIT 2009, 2009) provide recommendations concerning the visual qualitative approaches for the classification. According to the Italian Ministry of Infrastructures and Transportation (IMIT 2009, 2009), six types of patterns are defined (Fig. 7).

Type A Irregular stone masonry from river gravels
Type B Uncut stone masonry from external leaves of limited thickness and infill core
Type C Uncut stone masonry with good bond
Type D Regular masonry from soft sones (tuff or sandstone)
Type E Ashlar masonry with sufficiently resistant blocks (higher resistance than Class D)
E1 With mortar joints
E2 Without mortar joints
Type F Brickwork

Subsequently, each typology is classified by the Italian Department of Civil Protection into two groups based on the structural performance quality (GNDT/SNN, 2002).

Class I Irregularly arranged, poor quality masonry:

- High seismic vulnerability in the IP and OOP direction,
- Tendency for disaggregation and local mechanisms,
- Poor intrinsic resistance from bad mortar quality or frictional resistance.

Class II Regular texture, good quality masonry:

- Low seismic resistance in the IP and OOP direction,
- Provided sufficient constraints on monolithic OOP behaviour,
- Good intrinsic resistance is provided by strong mortar or frictional resistance.

Type A and B are assigned to Class I and Type D, E and F to Class II. Type C needs special considerations to be assigned to a class. Furthermore, the Italian code (GNDT/SNN, 2002) recommends values for mechanical properties corresponding to different types of masonry patterns, which is here not reported for brevity. Other effects, like mortar quality or transverse connections, are considered through correction coefficients. However, even though such a methodology provides useful information for practitioners who perform numerical simulations, it might hide limitations, neglecting differences that typically affect other sub-classes of masonry.

A further classification typically adopted in engineering practice provides differentiation based on the arrangement's rules and the level of dressing of the stone units (Kržan et al., 2015; B. Indian Standards, 1992; British Standards Institution, 1984) (Fig. 8).

A. Arrangement of stones
1. **Uncoursed:** Varying shapes and sizes of stones are used, no horizontal courses can be identified
2. **Coursed:** Stones with uniform height are placed in horizontal courses
3. **Brought to courses:** Horizontal courses are levelled at some intervals

B. Stone dressing
1. **Rubble:** Undressed or roughly dressed stones
   a. **Random:** Only the weak corners are removed with the masons' hammer
   b. **Squared:** Stones are roughly squared with a mason's hammer
   c. **Polygonal:** Stones are hammer dressed to have a polygonal shape
2. **Ashlar:** Accurately dressed, squared stones

One can note how the units' shape, arrangement and surface properties have a relevant influence on the structural behaviour of the HMS; however, the above classification neglects some crucial factors which are related to the structural behaviour of the HMS (Borri et al., 2015).

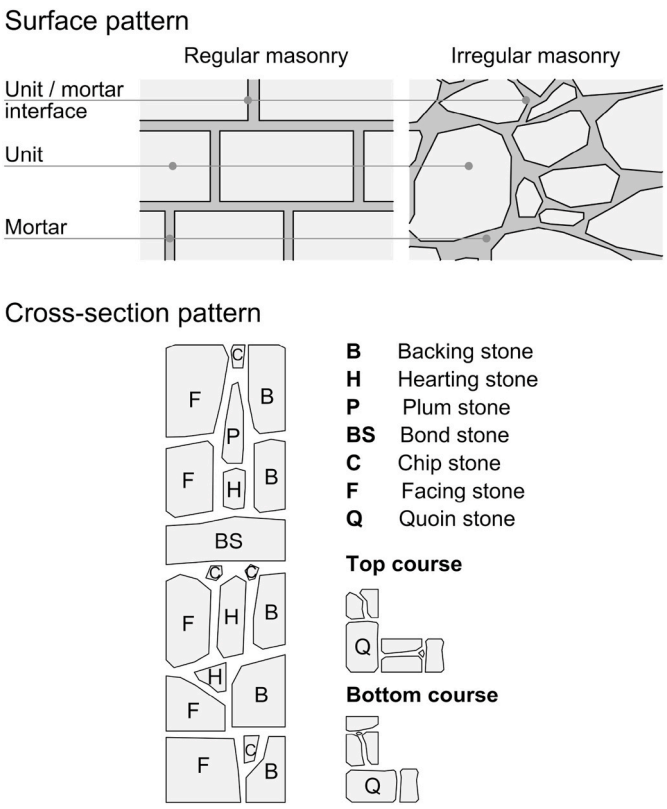

Fig. 5. Nomenclature of masonry units.

HMS does not always exhibit monolithic behaviour. Poorer infill materials were used through the thickness, affecting the mechanical behaviour of multi-leaf walls. Consequently, it appears clear how the classification of masonry patterns' cross-section deserves a detailed investigation (Quelhas Da Silva et al., 2014).

Based on the research work developed by Binda (Binda et al., 2005), three classes of masonry cross-sections can be identified by the number of leaves and a fourth by the filling of joints (Fig. 9). Class A contains single-leaf walls or walls with sufficient interlocking in thickness. Thus, the structure behaves monolithically in OOP failure. These walls are constituted by irregular or regular stone elements and are bonded together with thick, horizontally or sub-horizontally inclined mortar joints. Class B contains walls with two different leaves of stones. Further differentiation can be made by observing the connection between the leaves, which can be (i) continuous vertical mortar joint, (ii) nearly empty vertical joint or (iii) insufficient connection between the leaves. In Class C, walls with two external leaves are contained, separated by an internal rubble core. In some cases, the external leaves can be connected by *diatons*, since, in the opposite case, the lack of connection between leaves strongly reduces the load transfer between the external leaves. Finally, Class D contains stone masonries with dry joints. One should note that it is only meaningful to group the classes considering the morphological properties of the wall, which mainly influence the OOP behaviour (Fig. 9) (Kržan et al., 2015; Binda et al., 2005).

2.2. Masonry pattern's parametrisation with quality indexes

As previously mentioned, the structural behaviour of HMS generally depends on a large number of properties, such as the material properties, geometry of the constituents, assembly technique (with mortar or dry joints), quality of texture, the morphology of assemblage, conservation state of the materials, etc. (Kržan et al., 2015). Regarding the constituent elements, the response depends on the units' dimension, shape and dressing, the quality of the mortar joints, the presence of wedges, and the homogeneity of the constituent materials (Binda, 2001). Therefore, QI-s should be measurable from geometry, e.g. shape and size of units. At the same time, response measures (RM) should be calculated from the structural response, e.g. strength capacity or failure mechanism characteristics. The correlation between a set of QI-s and a selected RM estimates the structural response based on the properties of the masonry texture and, consequently, useful information concerning the structural performance of HMS.

Most of the literature examining the effect of masonry patterns deal with one specific problem by either considering the surface (IP loading) or the cross-section (OOP loading) pattern. For this purpose, only a limited number of parameters were usually used. Conversely, when multiple parameters were used, they were considered independent of each other (de Felice, 2011; Rios et al., 2022; Zhang and Beyer, 2019).

OOP behaviour of HMS can range from rigid-body overturning to disintegration (de Felice et al., 2022b). For this motivation, one of the aspects taken into account for masonry parametrisations aims to quantify the capacity to behave monolithically (which also corresponds to the I condition of the "rules of art"). The first attempt to quantify the monolithic behaviour was developed by Giuffrè (1990), who defined the interlocking parameter ρ_s, which is the ratio between the average vertical distance between *diatons* and the thickness of the masonry wall. He identified a linear correlation between load factor (λ) and *diaton* frequency (ρ_s) (Fig. 10).

$$\rho_s = \frac{d_s}{t} \sim \lambda \tag{1}$$

Afterwards, de Felice et al. (de Felice, 2005) refined the above method and recommended the use of the slenderness of the unbounded section of the wall by introducing a parameter a_χ, quantifying the lack of interlocking between leaves:

$$a_\chi = \frac{\beta_{local}}{\beta_c} \tag{2}$$

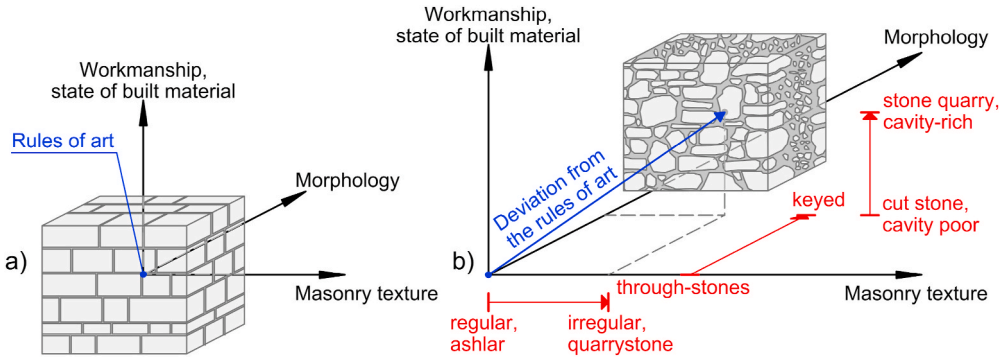

Fig. 6. Parameters for the improvement of the monolithic response of HMS (Kržan et al., 2015; Wigger et al., 2000).

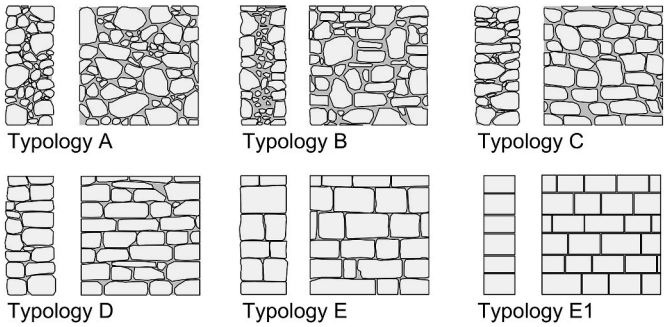

Fig. 7. Different stone masonry typologies according to the Italian standard (Vanin et al., 2017).

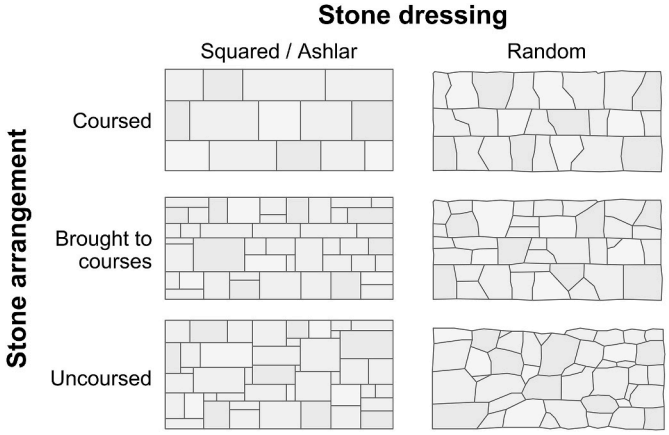

Fig. 8. Different rubble masonry typologies based on the dressing of stones and stone arrangement.

where $\arctan(\beta_c)$ is the global and $\arctan(\beta_{local})$ the internal slenderness of the wall's cross-section. β_{local} is selected from the most slender, unrestrained portion of the wall cross-section. Subsequently, the increase of a_χ corresponds to a decrease of the OOP capacity.

In order to measure the interlocking among units, Doglioni and Mirabella (Doglioni and Roberti, 2004) recommended the use of the indenting index (also called vertical line of minimum trace) M_l, which is defined in Eq. (3), as the line of least resistance (polyline with minimum length) through the mortar joints in a 1.0 × 1.0 m^2 window (Fig. 11). They recommended to use M_l for both the surface and the cross-section patterns and defined limit values for the classification of the masonry patterns. Zhang et al. (Zhang and Beyer, 2019) used the diagonal line of minimum trace (connecting the two opposite corners of the window) and observed a better correlation with the shear-compressive response than with the vertical one.

$$M_l = \frac{\sum_{i=1}^{n-1} \left\| \underline{p}_i - \underline{p}_{i+1} \right\|}{\left\| \underline{p}_{start} - \underline{p}_{end} \right\|} \tag{3}$$

Where $\underline{p}_{start}$ and $\underline{p}_{end}$ are the position vector of the first and last vertices of the polyline, while $\underline{p}_i$ refers to the *i-th* vertex.

Binda (2001) stated that voids could significantly reduce the interlocking between stones. Thus, the percentage of voids and their ratio with stone and mortar volumes are correlated with the OOP behaviour (Fig. 12). It was also experimentally observed that the injection of voids can significantly increase the structural capacity of the stone masonry (Binda et al., 1997).

Smaller units reduce the masonry's strength due to the stones' lower roughness, which governs the generation of frictional resistance. Furthermore, smaller units generally correspond to higher percentages of mortar volume, which reduces the structural strength. Thus the average size of the units is representative of the structural response. When the average size of units is considerable, relatively high strength is guaranteed, while if it is small, the strength is very scattered (Fig. 13) (de Felice, 2011). Performing parametric analyses on cross-sections made of rubble masonry, Angiolilli et al. (2021) concluded that increasing the size of the structure (or reduction of units) reduces structural strength and ductility.

To interpret the monolithic response of the HMS, Baggio and Carocci (Bernardi, 2000) suggested an index of masonry quality (IMQ_c), which measures the deviation of response from that of the overturning failure of a rigid block:

$$IMQ_c = \frac{\lambda_c \beta_c}{\lambda_m \beta_m} \tag{4}$$

where β_c is the aspect ratio and λ_c is the maximum load factor of the masonry cross-section. β_m andλ_m represent the same parameters for a monolithic block of similar slenderness. Then, the load factor of the homogeneous block can be calculated as:

$$\lambda_m = \begin{cases} B_c/H_c & \text{if } H_c > B_c/\tan\varphi \quad \text{Rocking overturning} \\ \tan\varphi & \text{otherwise} \quad \text{Shear failure} \end{cases} \tag{5}$$

where B_c and H_c are the width and height of the wall cross-section and φ the friction angle of the joints. If the wall is simply constrained at its base (cantilever boundary condition), then $IQM_c = 1.0$ represents monolithic overturning, while $IQM_c \approx 0.4 - 0.5$ corresponds to the separation of leaves and consequent overturning and mutual sliding of the leaves (Fig. 14).

For the surface pattern, the size, shape, and interlocking of units influence the structural response (corresponding to the II and III con-

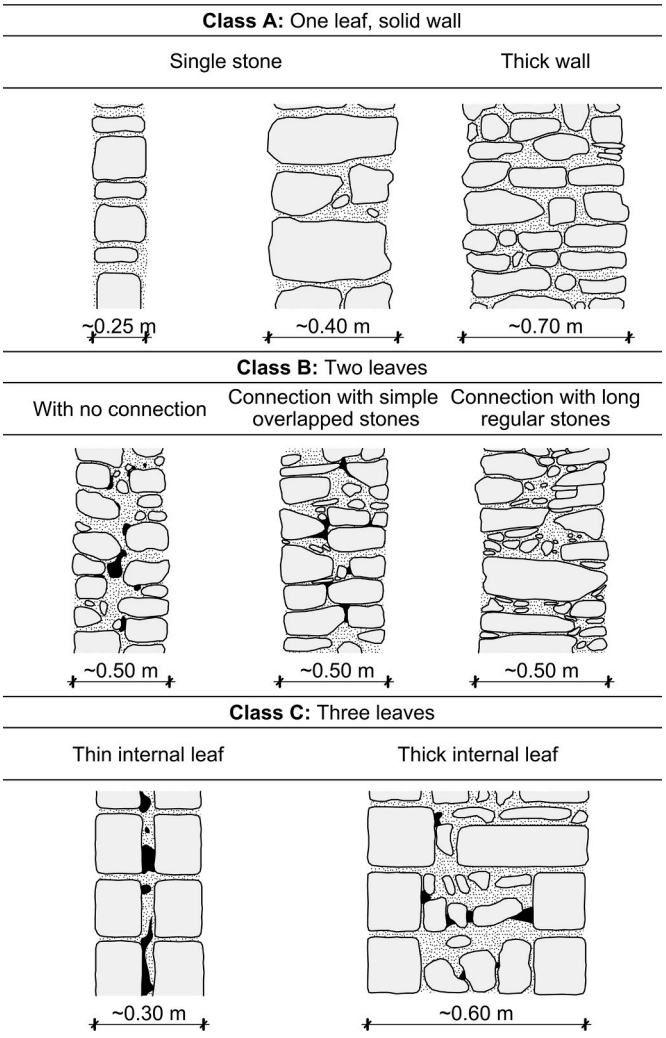

Fig. 9. Classification of masonry wall sections (Binda, 2001).

ditions of the "rules of art"). For rectangular-shaped blocks, the units can be characterised by the average slope of the bond α_b (Fig. 15) (Rios et al., 2022; Giuffre et al., 1994) and the aspect ratio β_b defined as (Binda, 2001; Angiolilli et al., 2021):

$$\beta_b = H_b / B_b \tag{6}$$

where H_b is the height and B_b is the unit's width. Subsequently, approaches have been proposed to represent irregular masonry as an *equivalent opus quadratum*, based on the equivalence of β_b and α_b (Giuffre et al., 1994; Funari et al., 2022a).

In order to take into account the joints effect of β_b and α_b, Malomo et al. (2021) introduced a geometrically inferred ratio a_{hj} over a representative volume element (RVE) of the pattern, which is not dependent on the assumption of rectangular units:

$$a_{hj} = A_b / A_{hj} \tag{7}$$

where A_b and A_{hj} are the area of units and head joints in the RVE, respectively. It is also well known from the analytical formulation of Mann and Müller (1982) that the shear capacity of the masonry structure is dependent on the slope of the lowest energy crack paths for the considered masonry pattern:

$$\tau = \frac{c}{1+\mu\varphi} + \frac{\mu}{1+\mu\varphi}\sigma_y \tag{8}$$

where c is the cohesion, μ the friction coefficient, σ_y is the normal stress and φ represents the tangent to the angle of the minimum energy crack path $\varphi = \tan(\alpha_b)$. For a regular bond pattern, the value of α_b can be easily calculated as:

$$\alpha_b = \arctan(2H_b / B_b) \tag{9}$$

Corresponding to the average value of the bond. In the case of irregular masonry, the value of α_b needs to be determined by statistical means over a representative area, either through the determination of the minimum diagonal crack path with a minimisation algorithm or by calculating the average ratio of overlapping lengths $2\overline{H_b}/\overline{B_b}$ (Fig. 15)

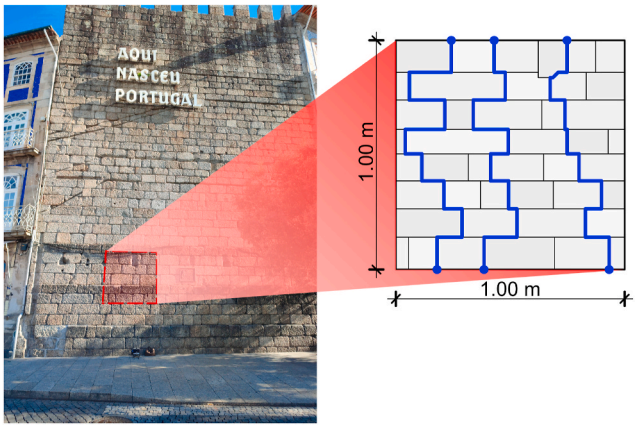

Fig. 11. Calculation of the indenting index of a surveyed masonry pattern (Doglioni and Roberti, 2004).

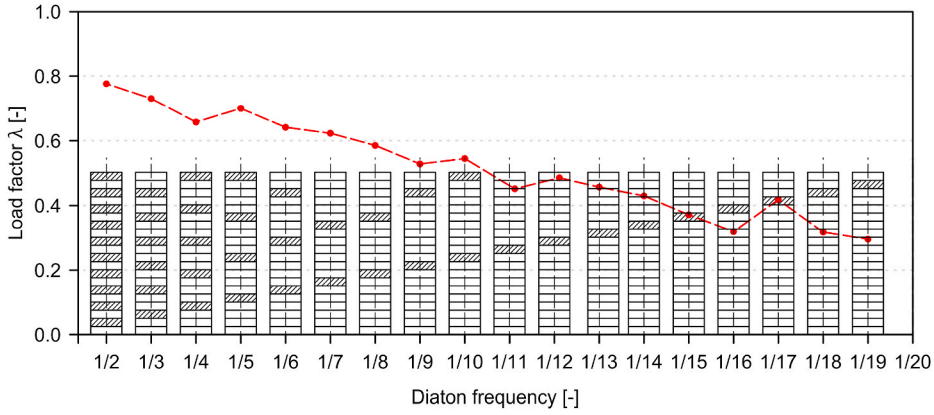

Fig. 10. Overturning strength related to the number of diatons (Giuffré, 1996).

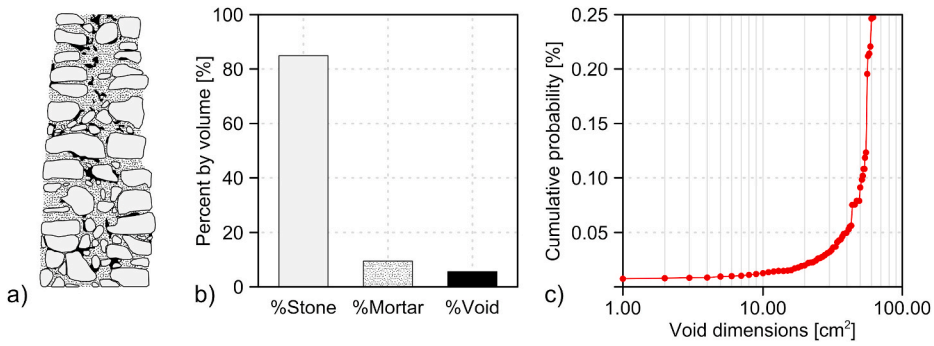

Fig. 12. a) Masonry cross-section with b) percentage of stones, mortar and voids andc) size distribution of voids (Binda, 2001).

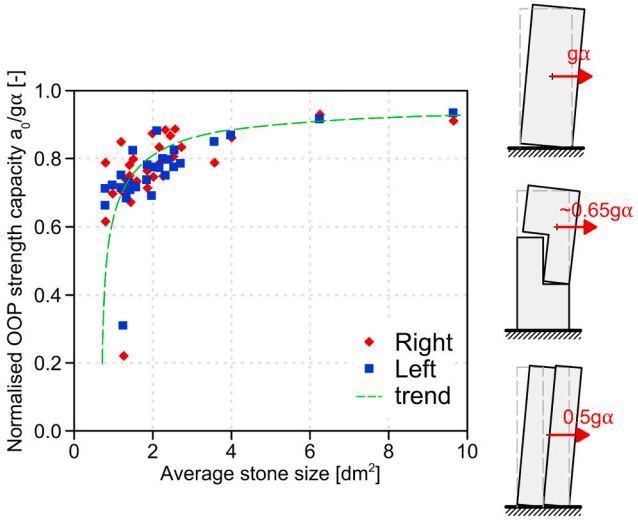

Fig. 13. Relationship between out-of-plane capacity and average unit size (de Felice, 2011).

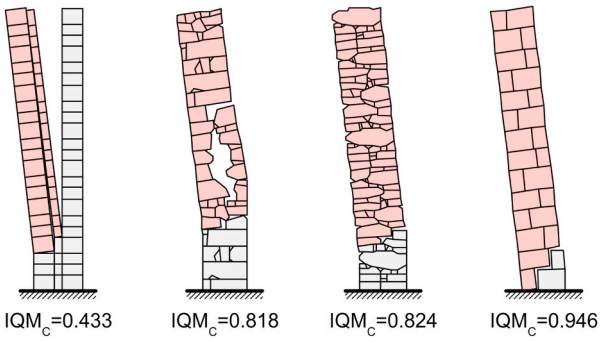

Fig. 14. *IQM* for different masonry cross-sections (Bernardi, 2000).

(Calderini et al., 2010). Macro LA formulations for regular patterns also use the parameter α_b which corresponds to the crack inclination for pure rocking failure mode (Casapulla et al., 2013). For irregular masonry patterns, the authors (Funari et al., 2022a) proposed the use of the structured path UP-RIGHT-UP-LEFT for coursed rectangular and the vertical (M_l) and horizontal ($M_{0,l}$) lines of minimum traces for rubble masonries. M_l takes into account the units' interlocking, while $M_{0,l}$ quantifies the reduction in shear resistance of joints due to the non-horizontal inclination of bed joints (Funari et al., 2022a; Szabó et al., 2022).

$$\alpha_b = \arctan\left(\frac{M_l - 1}{M_{0,l}^2}\right) \tag{10}$$

To quantify the deviation of the unit's shape (and orientation) from rectangular, the block area ratio (a_{block}) was introduced by Zhang et al. (Zhang and Beyer, 2019):

$$a_{block} = \frac{\sum_i A_{b,i}}{\sum_i A_{box,i}} \tag{11}$$

where $A_{b,i}$ is the area of a stone and $A_{box,i}$ is the minimum area, horizontally positioned bounding box around it. Almeida et al. (2016) identified a remarkable linear correlation between the shape of the units and the percentage of stones in a wall:

$$a_{stone} = \frac{\sum_i A_{b,i}}{A_w} \propto \frac{1}{a_{block}} \tag{12}$$

where $A_{b,i}$ is the area of a unit and A_w is the area of the considered wall. This suggests that masonry patterns with a lower percentage of stones tend to have fewer rectangular stones.

Borri et al. (2015) defined a methodology to correlate a masonry quality index (MQI), observed by visual inspections, with mechanical properties of the masonry walls (Corradi et al., 2003; D'Ayala and Paganoni, 2011). The MQI is obtained by calculating seven geometric and mechanical parameters, such as the material degradation state (SM), unit size (SD) and shape (SS), cross-section interlocking (WC), in-plane interlocking (VJ), the horizontality of laying surfaces (HJ) and mechanical characteristics of mortar (MM) (Table 1). These parameters

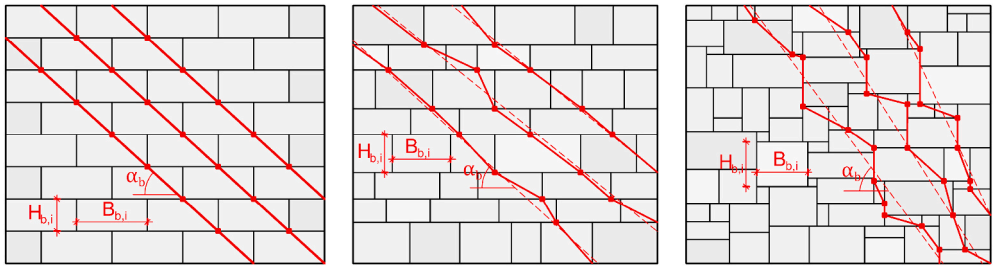

Fig. 15. Calculation of minimum energy path α_b for different masonry patterns (Calderini et al., 2010).

quantify independently of different aspects of the rules of art. Finally, the parameters are combined into one value with a weighted summation to obtain the MQI, which is subsequently correlated with the elastic, shear moduli, shear strength and friction coefficient (Marino et al., 2014) of the masonry structure, based on the recommendations of the Italian code (IMIT 2009, 2009) for usual masonry structures in Italy:

$$MQI = SM \cdot \gamma_{SM}(SD \cdot \gamma_{SD} + SS \cdot \gamma_{ss} + WC \cdot \gamma_{WC} + HJ \cdot \gamma_{HJ} + VJ \cdot \gamma_{VJ} + MM \cdot \gamma_{MM}) \quad (13)$$

The weights ($\gamma_{..}$) are dependent on the type of loading on the masonry structure (vertical, IP or OOP), taking into account that in different loading conditions, the geometric parameters have different influences on the response (Giuffre et al., 1994). The value of MQI can range from 0 to 10, where the higher value corresponds to a higher level of regularity. Furthermore, the masonries are classified into three behavioural categories based on their MQI (Table 2).

Inspired by the MQI method, Almeida et al. (2016) defined the masonry irregularity index (I_{FG}), which only considers the geometric characteristics of the masonry surface pattern:

$$I_{FG} = \alpha \cdot I_{FP} + \beta \cdot I_{DP} + \gamma \cdot I_{AH} + \delta \cdot I_{AV} \quad (14)$$

where I_{FP}, I_{DP}, I_{AH} and I_{AV} represent the stone shape, size and horizontal and vertical alignment factors, respectively (Fig. 16). For more details the reader can refer to (Almeida et al., 2016).

Using the approaches above, several researchers (de Felice, 2011; Rios et al., 2022; Zhang and Beyer, 2019) have observed that the weighted summation of parameters is inherently flawed since the interaction of some parameters is statistically significant. In particular, in coursed rectangular masonry, the pattern is characterised by a high level of interlocking; thus, the quality of mortar does not significantly influence the structural response, while in the case of rubble masonry, the interlocking of the pattern is generally lower, resulting in a higher influence of the mortar quality. This non-negligible interdependence of QI-s should be investigated via a multidimensional analysis tool, such as Principal Component Analysis to determine the most significant components or Analysis of Variance to assess the statistical significance of interaction terms. A further important aspect is the choice of appropriate RM. In the literature, the stiffness, peak load, residual lateral force capacity, displacement capacity, ductility and equivalent viscous damping are usually measured and numerically assessed. On the contrary, the failure mechanisms are only assessed qualitatively by the visual inspection of the crack pattern, damage in units, and relative displacements of components (Vladimir et al., 2011).

2.3. Masonry patterns' mechanical repercussions

As presented in Fig. 17, masonry structures with irregular patterns attain more severe damage than the ones with more regular patterns.

This section investigates the masonry pattern's influence by considering its relationship with the parameters defined in the previous section. In the case of IP actions, three basic crack patterns can be identified (Quelhas Da Silva et al., 2014; Almeida et al., 2014), which might evolve independently or in combination with each other (Fig. 18): (i) flexural failure, where flexural cracks form at the corners, and the wall behaves as a rigid block, rotating around the toe (at high vertical stress with toe crushing), (ii) shear-diagonal failure, with the formation of diagonal cracks developing from the centre of the wall and propagating towards the corners, (iii) shear-sliding failure, with the shear failure and subsequent sliding of the bed joints.

The occurrence of one failure mode rather than the other depends on the constituents' mechanical parameters (Gonen et al., 2021; Pulatsu et al., 2022), geometry, boundary (Casapulla et al., 2021; Restrepo Vélez et al., 2014; Vaculik and Griffith, 2017; Howlader et al., 2020), environment (Elghazouli et al., 2022a, 2022b; Guo et al., 2022) and loading conditions. Generally, rocking failure prevails in slender walls, while

Table 1
Masonry quality indexes and fulfilment conditions (Borri et al., 2015).

Id.	Description	Criteria		
		NF	PF	F
SM	Mechanical properties and conservation state	**Ratio of degraded elements**		
		> 50%	> 10%	> 10%
		Ratio of hollow bricks		
		> 70%	> 45%	> 45%
		Examples		
		Mud or unfired bricks	Sandstone. Tuff	- Solid brick - Concrete blocks - Hardstone
SD	Stone/brick dimension	**More than 50% elements with a larger dimension than**		
		< 20 *cm*	20 − 40 *cm*	> 40 *cm*
		Examples		
		Only head joints	Co-presence of different dimension elements	Co-presence of different dimension elements
SS	Stone/brick shape	**Examples**		
		Mostly rubble. Rounded or pebble stonework on both leaves	Co-presence of rubble and cut stones/bricks on both leaves	Barely or perfectly cut stones on both leaves
			One leaf from perfectly cut stone or bricks	Brickwork
WC	Wall leaf connections	**Qualitative (header density ρ_h)**		
		$\rho_h < 2/m^2$	$\rho_h < 2 - 5/m^2$ and header length is close to wall thickness	$\rho_h < 4 - 5/m^2$ and header length is the thickness of the wall
		Quantitative (line of minimum trace M_l)		
		$M_l < 1.25$	$1.25 < M_l < 1.55$	$M_l > 1.55$
HJ	Horizontal joint characteristics	**Examples**		
		Not continuous	- Intermediate - One leaf is continuous but the other isn't	Continuous
VJ	Vertical joint characteristics	**Wall with single leaf**		
		$M_l < 1.4$	$1.4 < M_l < 1.6$	$M_l > 1.6$
		Wall with two leaves		
		$M_l < 1.4$ for first leaf $M_l < 1.6$ for the other	Either both leaves: $1.4 < M_l < 1.6$ or one of the leaves: $M_l > 1.6$	Both leaves: $M_l > 1.6$
MM	Mortar mechanical properties	**Examples**		
		- Low cohesion mortar - No mortar (rubble) - Large bed joints or porous stones with weak mortar	- Medium quality mortar - Irregular masonry with weak mortar with pinning stones	- Non degraded mortar - Regular bed joint thickness - Perfectly cut joints with no mortar

Table 2
Masonry categories as a function of the MQI and the direction of action (Borri et al., 2015).

Category		Direction of action		
		Vertical	IP	OOP
A	Good behaviour	≥ 5	≥ 5	≥ 7
B	Average behaviour	$2.5 \leq MQI \leq 5$	$3 \leq MQI \leq 5$	$4 \leq MQI \leq 7$
C	Inadequate behaviour	≤ 2.5	≤ 3	≤ 4

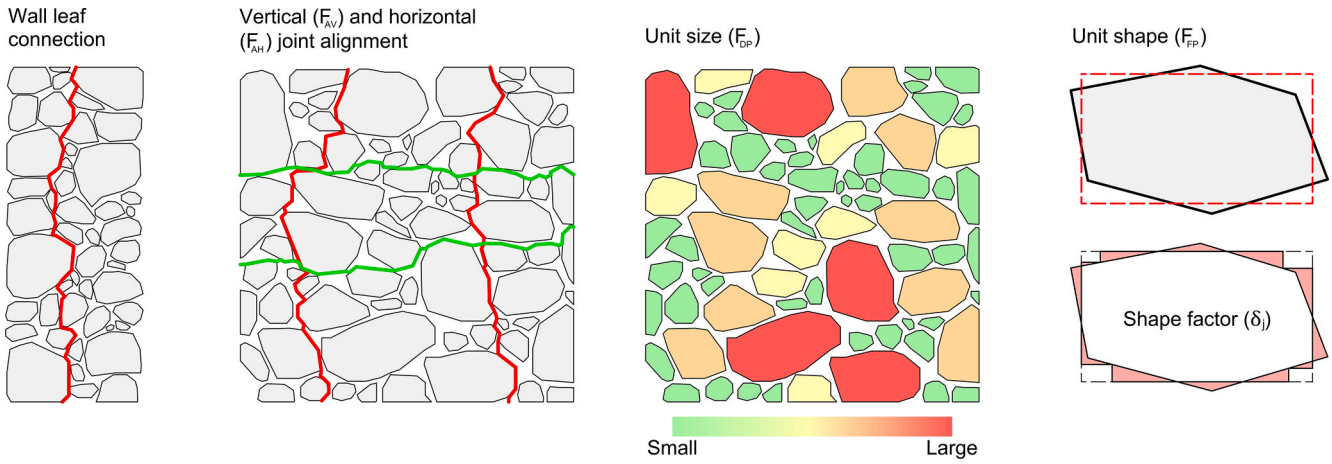

Fig. 16. Masonry quality parameters defined by (Borri et al., 2015; Almeida et al., 2016).

bed joints sliding is usually observed for squat walls. Under low pre-compression, the structures usually fail due to flexural failure, while with the increase of overload, the shear crack starts dominating the failure (Vasconcelos and Lourenço, 2009). As the overload or the mortar-to-stone strength ratio increases, the diagonal cracks go through stones rather than following the mortar joints causing units' crushing (Quelhas Da Silva et al., 2014). While some approaches rely on the rigid body failure of masonry walls under IP loading conditions (Funari et al., 2021a), the assumption that the masonry wall fails with the separation into one or two rigid blocks along a crack line passing through the point of rotation or sliding is not always satisfied since it depends on the masonry pattern.

Giuffrè (Giuffre et al., 1994) conducted experimental and discrete numerical parametric analysis on the shear-compressive response of dry joint, regular bond pattern masonry walls with different unit aspect ratios and boundary conditions. The walls subjected to only self-weight and increasing lateral loads did not behave in a rigid body motion but failed due to diffuse sliding (Fig. 19a). The presence of vertical loads emphasised the monolithic behaviours of the wall (Fig. 19b). Such a result was still more remarked in cases of horizontal connection along the top portion of the wall; even masonry with poor interlocking behaved monolithically (Fig. 19c). When eccentric vertical loading was present, and the friction coefficient (μ) was larger than the load factor associated with the pure rigid body failure (λ_{rigid}), then it failed performing a rigid body motion and $\lambda = \lambda_{rigid}$, while if the friction coefficient was smaller, then the wall exhibited a pure distributed sliding failure mode and $\lambda = \mu$ (Fig. 19d).

While it can be assumed that the joints of HMS have negligible tensile strength, the interlocking between blocks and their frictional contacts produces a pseudo-tensile strength governed by the compressive stress on the contact surface, the friction coefficient and the arrangement of blocks (Giuffré, 1996; Chen and Bagi, 2020). The pseudo-tensile strength influences the crack line's angle of inclination that causes collapse. As illustrated in Fig. 20, higher IP interlocking levels generate larger crack inclinations. It is also presented that the failure mode can change from overturning to sliding depending on the friction coefficient.

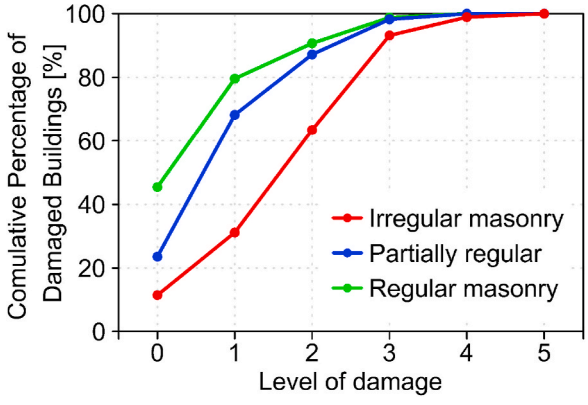

Fig. 17. Post-earthquake assessment of the existing building stock of Norcia after the 2016 central Italy earthquake (Borri et al., 2020).

If the structure fails with material disaggregation, methods based on the macro element assumption overestimate the strength and displacement capacity. Borri et al. (2020) observed how the condition $MQI < 4$ for OOP load leads to disaggregation. The main factors are poor quality mortar and bad connections between leaves and non-horizontal bed joints. Generally, random rubble masonry has a high chance of disaggregating, but the presence of good mortar quality almost guarantees no disaggregation. If the mortar quality is poor, the presence of horizontal bed joints and proper connection of leaves can prevent disaggregation. Properly dressed masonry is prone to disaggregation only if the quality of mortar is very weak and the leaves are not correctly connected. Squared stone masonry rarely fails by disaggregation because the shape of the units always provides the horizontality of bed joints and proper leaf connection.

Zhang et al. (Zhang and Beyer, 2019) analysed five typical Italian masonry typologies via numerical analyses and correlated the results with three different QI-s (vertical and diagonal lines of minimum trace and block area ratio). At a low level of pre-compression flexural failure occurred, and no correlation between the shear strength and the QI-s was found. It is because the geometry of the wall and the kinematic boundary conditions only control the failure. However, a clear correlation between the QI-s and the shear strength was observed in the case of shear failure. Although the correlation was quite scattered, the diagonal line of minimum trace ($M_{l,d}$) showed the best correlation with the shear strength.

In the same research work (Zhang and Beyer, 2019), the effect of unit shape was examined by comparing the behaviour of wall panels with rectangular and elliptical-shaped units. The rectangular pattern's shear capacity increased by decreasing β_b, while the elliptical's slightly decreased. Although M_l changed significantly, the shear capacity remained constant. Considering β_b constant and gradually changing shape from elliptical to rectangular, a linear correlation has been observed between the a_{block} and the shear capacity. As the unit shape tended from rectangular to elliptical, the failure mechanism changed from flexural to pure shear, while the compression struts tended from diagonal to vertical. In the case of low values of β_b with thin mortar joints, the properties of the head joints did not influence the shear strength, but in the case of close to square units and thick mortar joints,

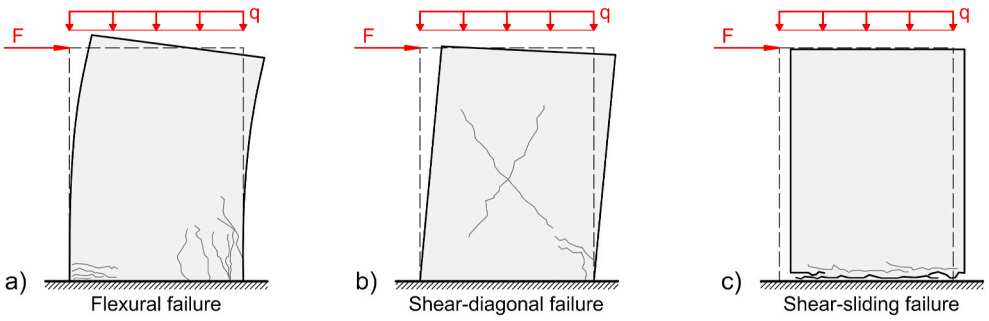

Fig. 18. The three basic in-plane failure modes of masonry walls (Calìò and Pantò, 2005): a) flexural failure, b) shear-diagonal failure, c) shear-sliding failure.

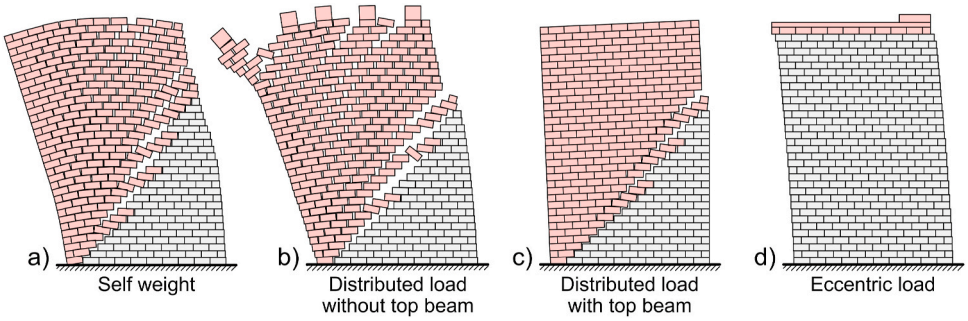

Fig. 19. Collapse mechanism of shear wall under different boundary conditions and overloads (Giuffre et al., 1994).

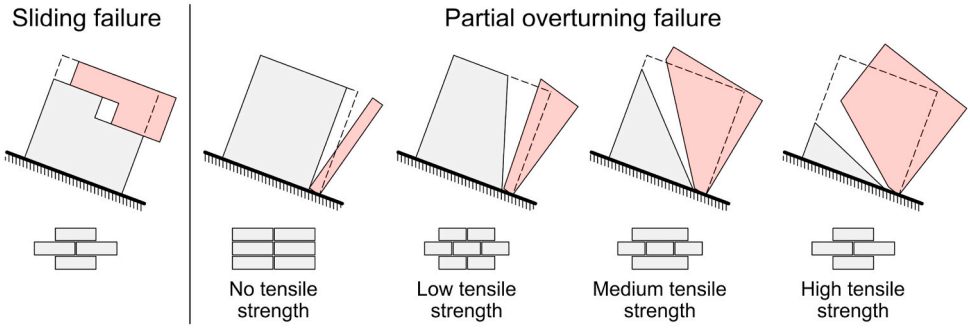

Fig. 20. In-plane failure mechanisms of shear walls with different levels of interlocking (Giuffré, 1996).

it had a non-negligible effect. Indeed, it has also been experimentally demonstrated by Maheri et al. (2011), that both stiffness and capacity IP and OOP of masonry walls can deviate from 30 to 50% as the degree of filling of the head joints varies. The change in unit elastic properties provided negligible differences in the shear capacity. Lower tensile fracture energy decreased the shear capacity, even though this effect decreased as the vertical loading increased. As the size of the wall increased, the shear capacity subsequently decreased, showing a clear indication of the panel size effect. In this framework, Angiolilli et al. (Calderini et al., 2010) experimented that increasing the wall size decreases masonry structures' structural strength and ductility.

Malomo et al. (2021) conducted parametric DEM analyses on masonry walls with different bond types (Flemish, English, Dutch cross-bond, header and running bonds). The results were validated with experimental results, which showed good agreement in the strength capacity and slight differences in the failure modes generated by the spatial variation of mechanical properties (Zhang and Beyer, 2019; Angiolilli et al., 2021; Zhang et al., 2017). As the shear span ratio α_v (ratio of wall height and the shear span) increased, the initial stiffness also increased, and the stiffness difference between different bond types decreased. β_b had the most significant effect on the initial stiffness, with more slender units having higher initial stiffness and smaller differences between different bond types. It has been observed that the order of stiffness and a_{hj} parameter values corresponding to the different bond types were the same, thus a_{hj} can be an adequate parameter to characterise the stiffness of the bond types. The peak shear capacity was increased by α_v and decreased by axial load ratio σ_L (ratio of pre-compression and unit compressive strength), while the bond type did not have a significant effect. The bond type and α_v had a significant impact on the type of activated failure mechanism, thus, subsequently, on the displacement capacity, while the effect of σ_L was not evident. RUN and FLE patterns have exhibited top and bottom sliding while ENG, DUT and HEA failed in diagonal shear prematurely. The difference in displacement capacity of different bond types was larger as β_b increased. The extent of parallel stepped cracks was inversely proportional to a_{hj}, which reduced the displacement capacity and corresponded to a more brittle failure mode. Brick crushing ias observed in walls with high β_b. It should be noted how Rios et al. (2022) showed that the interaction between all the above-considered factors, except between the unit aspect ratio and the bond type, has a non-negligible effect on the response.

An experimental campaign of quasi-static cyclic tests on (i) dry stack

Table 3
Summary of the experimental failure modes of masonry test specimens (Vasconcelos and Lourenço, 2009).

Specimen specifications		Vertical compression [MPa]		
		0.5	0.875	1.25
R	Dry joints. Regular bond pattern	Rocking	Rocking/rocking and toe crushing	Rocking and toe crushing
IR	Coursed masonry with irregular stones	Rocking/flexural	Flexural/toe crushing	Flexural/toe crushing/shear
RB	Uncoursed random rubble masonry	Flexural/shear – flexural/rocking	Shear – flexural/shear	Shear

stone masonry with sawn cut units, (ii) irregular masonry with mortar and well-defined courses, (iii) random rubble masonry was conducted by Vasconcelos et al. (Vasconcelos and Lourenço, 2009). The failure mechanisms are presented in Table 3. Dry joint walls with regular bond patterns failed as the shear resistance of the bed joints was exceeded, and diagonal stepped cracks formed with the subsequent rotation of the upper part of the wall. Flexural response and rocking mechanism governed irregular coursed masonry walls at low and moderate pre-compression levels, while for lower pre-compression levels, horizontal cracks formed at the base of the wall, progressively spreading along the height. They found that rubble masonry walls are more dependent on the pre-compression level than the other typologies. Flexural behaviour and rocking mechanism characterised the response at low pre-compression levels, with smeared inclined cracks in the middle of the wall. At intermediate levels of pre-compression, no substantial damage could be seen until large diagonal shear cracks formed along the joints. At the highest level of pre-compression, diagonal shear cracks developed with the damage of stones and crushing of the upper and bottom corners of the wall. In all the cases, large stiffness degradation was observed.

Considering the differences between the bond patterns, the authors observed that the ductility, energy dissipation, and displacement capacity depend significantly on the masonry texture. Irregularities result in a decrease in ductility, and the pre-compression effect on the failure mechanism increases with the irregularity of the pattern.

Cyclic shear-compressive experimental tests were conducted by Almeida et al. (2014) on large stone block masonry walls typical in the northern region of Portugal. The pre-compression positively influenced the strength capacity in all the typologies, while no clear trend was observed for the displacement capacity (Fig. 21). The strength capacity also increased with the geometric regularity of the masonry (decreased with the irregularity index I_{FG}), while for the displacements, again, a clear trend could not be identified. High shear capacity does not correspond to high displacement capacity.

In all typologies, the ductility was reduced by increasing the pre-compression, but the correlation between ductility and masonry pattern irregularity is not clear. The stiffness of the wall decreased with the increase of irregularity of the bond, and higher energy dissipation corresponded to more irregular textures.

Seismic action can cause the OOP overturning of facades if their slenderness and connection to side walls are inadequate. De Felice et al. (de Felice et al., 2022a) conducted a 2D DEM numerical analysis campaign on masonry churches damaged in the 2009 L'Aquila earthquake (Fig. 22). Static pushover and dynamic pulse excitation analyses were conducted. Fig. 22 compares the failure mechanism and capacity curves obtained from DEM and rigid body method (RB) in different churches.

The church in Fig. 22a is constituted by a regular, good-quality pattern in the façade, while relatively poor quality in the sidewall, resulting in the formation of a vertical crack at the edge of the façade. Results between the two methods show good agreement because the rotational hinge and the participation of the side walls in DEM are close to that assumed by the RB method. In the churches represented in Fig. 22b the masonry patterns can prevent the complete detachment of the façade, thus increasing the capacity. In this case, RB method underestimates the capacity since the rotational hinge is higher than the base of the wall and part of the sidewall participates in the mechanism. One should note how the sidewall effect is highly dependent on the ratio of its thickness with the thickness and span of the façade. As reported in Fig. 22c, in the case of poor sidewalls' masonry quality, the retaining

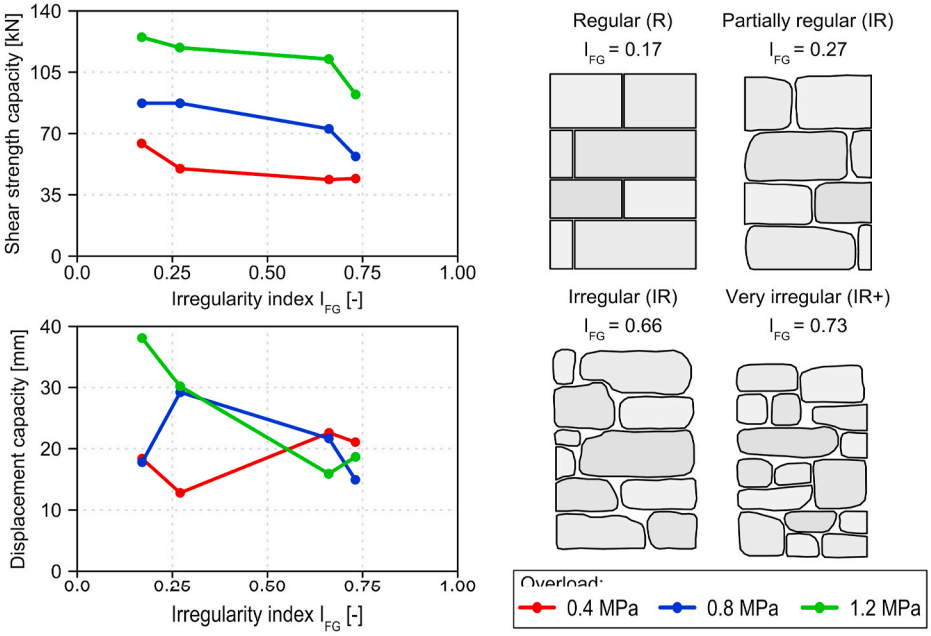

Fig. 21. Shear and displacement capacity for different masonry samples and pre-compression levels (Almeida et al., 2014).

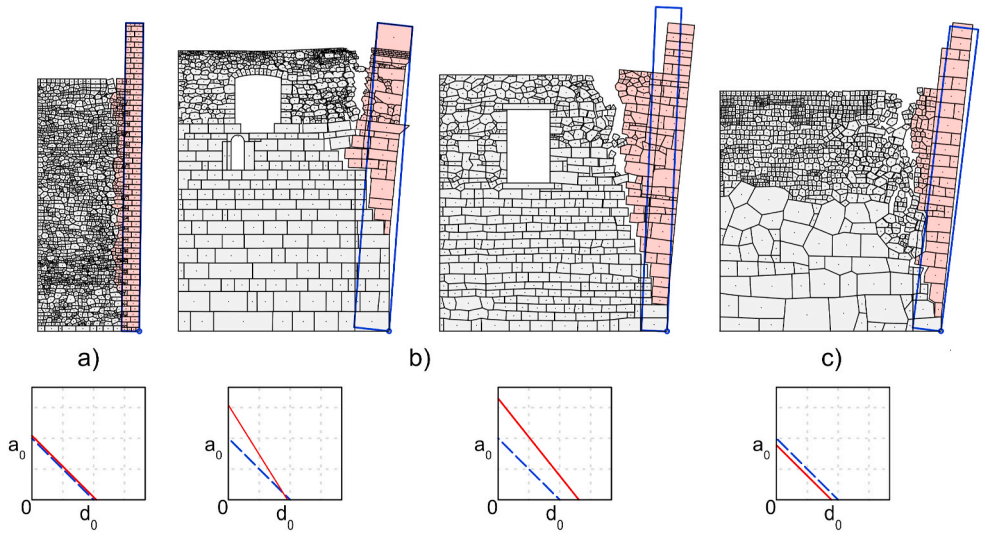

Fig. 22. Comparison of failure mechanisms obtained from the discrete element method (green) andrigid block rocking dynamics (red) (de Felice et al., 2022a). (For interpretation of the references to colour in this figure legend, the reader is referred to the Web version of this article.)

walls played a negative effect since they apply a thrust force on the façade. In this case, the RB method overestimates the capacity of the church. Dynamic investigations demonstrated how the variation of the pulse period did not significantly influence the failure mechanism and the acceleration capacity of the structure, proving that the response is mainly controlled by the geometry of the church and not by the seismic input (de Felice et al., 2022a).

The same research group performed a shaking table test on the OOP dynamic response of random rubble masonry walls (de Felice et al., 2022b). The specimen was constrained horizontally at the top to simulate the floor connection. Firstly, vertical cracks were observed in the middle of the wall, indicating the initiation of separation of the leaves. Subsequently, a partial collapse occurred involving parts of the first leaf, involving the left side profile and the front face cracks. The total collapse of the wall was due to the separation of the front and back leaf, forming a horizontal crack around ¾ of the height of the wall and collapsing with a two-block out-of-plane vertical bending mechanism (de Felice et al., 2022b). The geometry of the rubble masonry was shown to have a significant effect on the response, enhanced by the presence of the weak mortar, resulting in the better suitability of discrete models than continuous ones (de Felice et al., 2022b).

A further critical mechanical repercussion derives from the leaves' morphology and mechanical characteristics. Especially the connection between leaves can highly influence their behaviour. The structural behaviour is bounded between Fig. 23a, where the wall is constituted by one leaf or the leaves are well connected; thus, it behaves like a monolithic block and Fig. 23b, where a vertical joint realises the connection between leaves resulting in no load transferred among leaves (Binda et al., 1994). Typical HMS's structural behaviour is placed between these two limit cases based on their morphological properties. Bad-quality masonry can also disintegrate at the top of the wall where the normal forces are relatively low, resulting in a lower strength and displacement capacity (Fig. 23b) (Leslie et al., 2017).

Binda et al. (Carbonara, 1996) conducted an experimental campaign for two leaves masonry walls. They remarked how the vertical joints behave more fragile when the loads are transferred by a compression-flexural mechanism (interlocking). In the case of good interlocking, the shear strength of the vertical joints mainly depends on the stones' mechanical characteristics. Even 7% of *diatons* in the cross-section can provide monolithic cross-section behaviour. Good quality mortar can ensure monolithic behaviour, but usually, weak mortar is present in HMS and time degradation further decreases its strength (de Felice, 2011; Borri et al., 2020). In the two limit states, either the leaves are connected by stiff transversal elements, which transfer the loads between leaves proportional to their axial stiffness, or the leaves are only loosely connected (collar joints or by infill rubble), in which case the load distribution between leaves is highly dependent on the bond strength between the constituents (cohesion and friction between the leaves) (Binda et al., 1991).

De Felice et al. (de Felice, 2011) conducted numerical DEM simulations of masonry cross-sections for static pushover and dynamic pulse excitations. No single QI could be identified that accurately predicts the seismic vulnerability of the wall cross-section, but close to monolithic overturning could be ensured if the indenting index (vertical line of minimum trace through the cross-section) was higher than 1.5 or at least 7% of *diatons* were evenly distributed in the cross-section. While for small or average stone size, the strength capacity of the walls was very scattered, larger stones provided a relatively high OOP resistance (Fig. 13). Most wall specimens failed due to overturning around a hinge for both static and dynamic analyses. In the case of inadequate transversal connection, both the strength and displacement capacity were highly reduced compared to monolithic behaviour. In some cases, especially in the case of three-leaf walls, the dynamic and static analysis provided very different results, while the pushover analysis resulted in overturning failure, with high strength and low displacement capacity, due to pulse excitation, the wall failed by separating the outer leaves and with a much lower strength capacity than static analysis (de Felice, 2011). Usually, the strength and displacement capacities are reduced by 25–30%, compared to a rigid block. If the reduction is more severe, then the failure is characterised by the separation of the leaves and has to be modelled by dynamic analysis.

2.4. Survey of masonry patterns via NDT

According to state-of-the-art recommendations (International Charter for the conservation, 1964; The Charter of Krakow 2000, 2000), destructive testing and invasiveness must be avoided to conserve historical and cultural values. However, allocating more resources for reaching a good knowledge level (KL), i.e. having a detailed knowledge of the geometrical and mechanical characteristics of the structure under investigation, allows less conservative assessment (Caprili et al., 2017). This underlines the importance of proper geometric surveying as an integral part of the conservation project (Valero et al., 2018; Binda and Saisi, 2009). In the case of global structural assessment, knowledge of the level of connection between structural members and of the quality of masonry texture is fundamental, which, as demonstrated in Section 2.3,

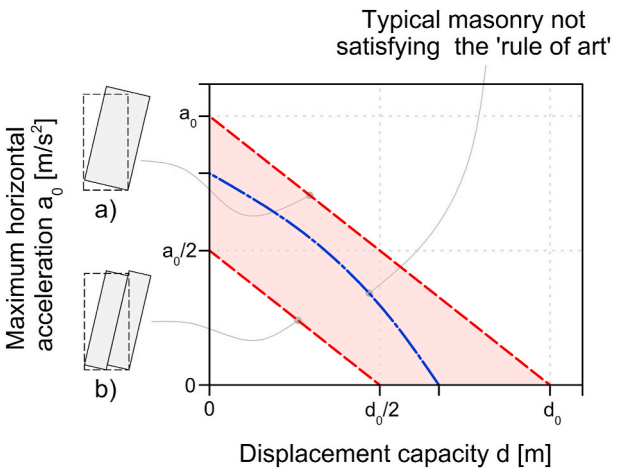

Fig. 23. Capacity curves for out-of-plane overturning depending on the connection of leaves (Giuffré, 1996).

significantly influences the structure's structural behaviour.

Several survey techniques might be employed to identify naked or plaster-covered surfaces or cross-section patterns. For example, if the wall is not covered by a plaster layer, terrestrial laser scanning (TLS) or digital photogrammetric (DP) techniques can be employed to survey the surface pattern.

The above techniques can provide a point cloud or image of the pattern, which has to be post-processed to acquire useful information for the structural assessment. However, the manual post-processing of the data is very tedious and time-consuming. For this motivation, automatic algorithms have been developed to assess the data. Algorithms usually use the 3D position or colour data to segment the point cloud (Sithole, 2008). Recently, more sophisticated deep learning-based segmentation algorithms have been developed, providing excellent results (Ibrahim et al., 2019). The outcomes of the detection algorithms can also be used in post-processing to calculate the width and depth of mortar joints to detect where repair is needed or areas where pinning stones (wedges) are recommended can be automatically detected (Casapulla et al., 2021).

When a plaster layer covers the wall's surface, it has to be removed in a small area, or NDT should be employed to survey the masonry behind the plaster. For instance, Ground Penetration Radar (GPR) utilises high-frequency electrical waves which reflect at the boundaries of different materials, can detect shallow objects in the structure, so the geometry of the surface features can be directly analysed (Lombardi et al., 2021). Infrared Thermography (IRT) uses a thermal camera to detect the wall's morphology, air leakage sources, heat losses, and moisture content (Bosiljkov et al., 2010). Acoustic Emission Technique (AE) detects the high-frequency elastic waves produced by the masonry fracture processes, which are subsequently analysed to interpret the damage location and severity on the structure (Verstrynge et al., 2021). Both GPR and IRT techniques provide only surface knowledge since the cross-section cannot be detected. Therefore, the complete surveying of morphological properties of multi-leaf walls cannot be performed in a non-destructive manner (Kržan et al., 2015). A combination of sonic and GPR tests, combined with coring, can be employed to identify multiple leaves. Large voids and inclusions of different materials can be detected with IRT, when they are near to the surface of the structural element. Deeper areas can be reached with GPR and sonic testing. Test on the moisture content can give valuable information on the degradation state of the masonry (Binda and Saisi, 2009). Masonry cross-sections can also be investigated by means of borescopy. A borehole can be drilled where a small camera can be inserted, allowing the detailed examination of the surface of the hole (Binda et al., 1997). One can note that the ideal condition for achieving the cross-section survey requires removing stones and directly surveying through the thickness. However, such an application is forbidden for heritage structures (Binda et al., 2005).

It is worth of point out that morphologic properties can usually be investigated by the combination of NDT and minor destructive (MD) methods (Table 4), while the characterisation of mechanical properties requires both in-situ and laboratory tests (Kržan et al., 2015; Arêde et al., 2019).

2.5. Masonry patterns generation

The lack of numerical research on irregular masonry patterns can be accounted by the difficulty of generating numerical modelling of irregular masonry typologies (Zhang and Beyer, 2019). Indeed, a limited number of masonry texture generator algorithms have been proposed in the literature. Mainly, the difficulty stems from varying the masonry pattern within specific criteria (Almeida et al., 2016). Generally, the algorithms are based on the probabilistic assumption that the dimension of the masonry units are unknown and can only be defined with certain statistical distributions:

$$D_n = D_{n0}(1 + \sigma_{Dn} \cdot N_x) \tag{15}$$

where D_{n0} is the mean and σ_{Dn} is the standard deviation of a dimension measure and N_x is a random variable following a predefined statistical distribution (usually normal distribution). Thus, the blocks are generated and placed in an order defined by the generation algorithm, constructing the masonry pattern.

A simple 2D pattern generator algorithm was recently presented by Vadalà et al. (2022). It can generate coursed rectangular masonry patterns defined by a random distribution of the unit widths and course heights (Fig. 24). The algorithm inputs are the minimum and maximum values of the number of units in a row, width, and height. The dimensions of the blocks are calculated according to Eq. (15). Furthermore, quoin stones, with predefined widths, can be defined at the ends of the masonry walls.

Cusatis (Angiolilli et al., 2021; CusatisZdeně et al., 1061) proposed an algorithm suitable for rubble masonry, where the input data are the minimum and maximum particle size, their distribution, the stone-mortar, water-mortar ratios and mortar content. First, spherical particles are generated in a specified volume (Fig. 25a), and then Delaunay tetrahedralisation is performed to define the interactions between particles. Finally, a domain tessellation is defined to create the faces of the units (Fig. 25b). The variation of mechanical properties of irregular masonries can be quantified with lattice discrete particle modelling (LDPM) because of its intrinsic stochastic nature. The method was also verified for modelling OOP loading (Ibrahim et al., 2019). However, the validation framework involved case studies with suspiciously monolithic behaviour.

A 2D masonry generator algorithm was proposed by Zhang et al. (Fig. 26) (Zhang et al., 2018), extending on the previous work of Miyata

Table 4
Investigation of morphological properties through ND and MD tests (Kržan et al., 2015; Bosiljkov et al., 2010).

Morphologic properties	Appropriate ND and MD methods				
	ND1	ND2	ND3	ND4	MD1
Thickness of the structural element			×	×	×
Detection of leaves and their thickness			×	×	×
Location of detachments of the outer layer			×	×	×
Investigation of the homogeneity of the masonry		×	×	×	
Location of larger voids		×	×	×	
Investigation of masonry pattern behind plaster	×		×		

N1 –Thermography, N2 – Sonic test, N3 – Radar, N4 – Ultrasonics, M1 – Endoscopy.

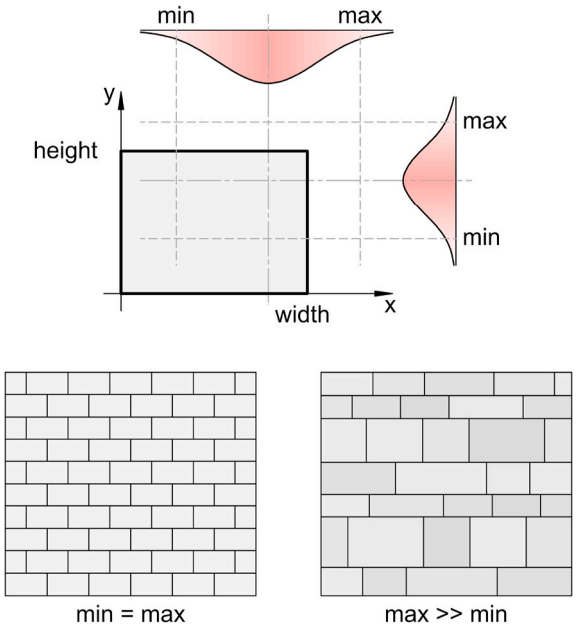

Fig. 24. Steps of pattern generation by Vadalà et al. (Vadalà et al., 2022).

(1993). Both generation algorithms can generate masonry patterns from regular to rubble masonry bond patterns. A synoptic representation of their algorithm is represented in Fig. 26.

Recently, a 3D masonry pattern generator has been proposed by Shaqfa (Shaqfa and Beyer, 2022), able to generate multi-leaf masonry walls ranging from rouble to regular. The algorithm consists of the generation of boxes with random dimensions, calculated by Eq. (15), and they are placed in a position determined by a constrained packing optimisation problem, which mimics the building process of the mason (Fig. 27). The placement of stones is calculated with the minimisation of an objective function, comprised of the weighted sum of three parameters, namely: (i) distance between the current and previous units (reducing the travel distance of the mason), (ii) vertical staggering of the head joints (good interlocking) and (iii) horizontality of the laying surfaces (good vertical stress distribution). Once all the boxes have been placed, they are substituted by synthetically generated, complex stone shapes and the voids are filled with mortar.

It is worth underlining that most of the developed generators are suitable for specific masonry typologies, whereas even the most general frameworks cannot systematically cover the all masonry typologies range. Furthermore, all the generators mentioned above are driven by the principle defined in Eq. (15), resulting in various masonry patterns orphaned of mechanical meaning since no adequate parametrisation as defined in Section 2.2 were considered. Therefore, proper parameters such as QI-s should be included in the generation algorithms to correlate

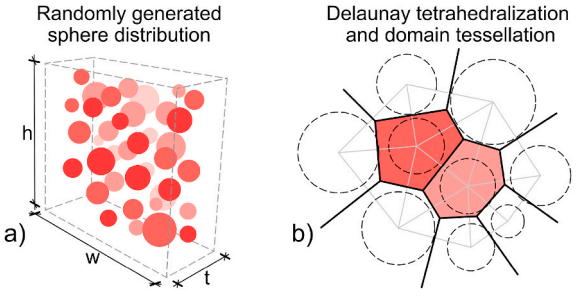

Fig. 25. Rubble masonry generation by Cusatis et al. (Angiolilli et al., 2021) a) Randomly generated sphere distribution and b) failure planes around the particles (Rios et al., 2022).

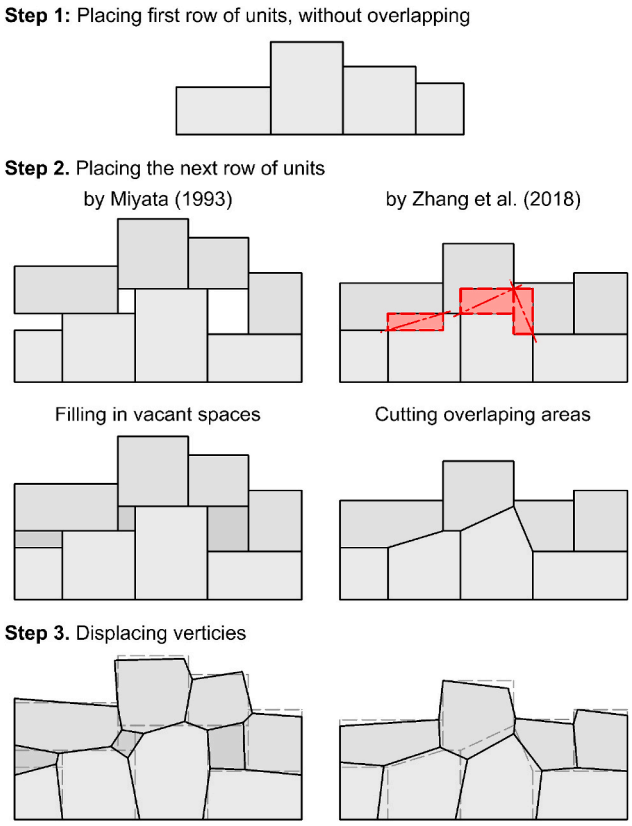

Fig. 26. Pattern generation by Zhang (Zhang et al., 2018) and Miyata (Miyata, 1993).

the structural response and the generated masonry pattern.

3. Comparison in terms of masonry textures generated following different approaches

The artificial generation of patterns plays a fundamental role in assessing the influence of masonry textures. In fact, ancient masons' skillset was reflected in their capacity to allocate masonry units, respecting a certain range of deviations from the "rules of art". Therefore, as the outcome of the above-presented literature review, the following research questions might be posed:

RQ1: What is the correlation between the overall quality of the

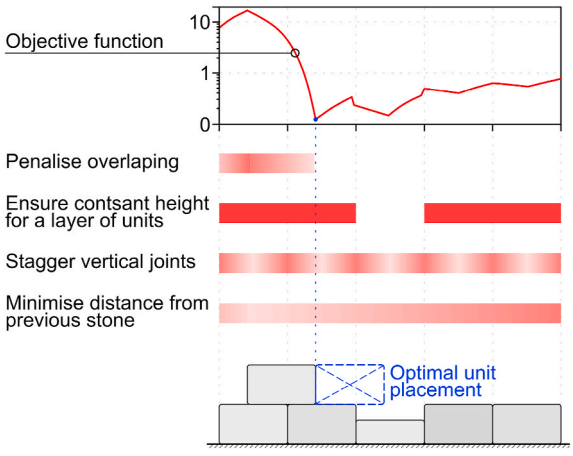

Fig. 27. Placement rule of units following the objective function (Shaqfa and Beyer, 2022).

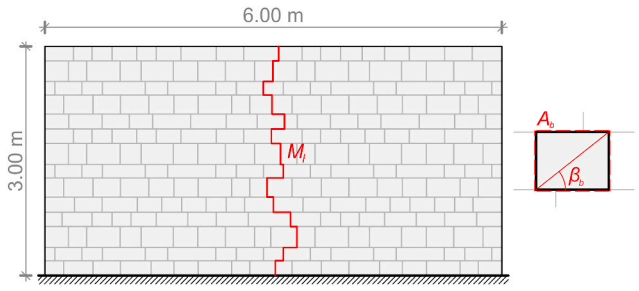

Fig. 28. Geometry and QI-s of the shear wall specimen considered in the parametric study.

masonry pattern and the structural performance?

RQ2: Can we systematically reduce the number of in situ tests increasing the knowledge about the correlation between masonry quality and RMs?

To this end, a preliminary parametric study has been developed, carrying out 2D pushover analyses of single-leaf shear wall specimens. Each specimen is defined by a rectangular wall panel of 6.00 × 3.00 × 0.20 m^3 in size with a coursed rectangular masonry pattern (Fig. 28). The masonry patterns are characterised by three QI-s, namely: (i) block area A_b, (ii) block aspect ratio β_b and (iii) vertical line of minimum trace M_l.

Throughout the analysis, three levels of pattern quality ($\{A_b\ [cm^2], \beta_b\ [-], M_l\ [-]\}$) are considered:

- Low $\{135, 0.54, 1.45\}$
- Normal $\{175, 0.44, 1.60\}$
- Good $\{215, 0.34, 1.75\}$

The Normal quality pattern has been chosen according to average values, according to (Baggio and Carocci, 2000; Binda et al., 1999), while the Good and Low quality patterns have been acquired with a consistent addition or subtraction from all three QI-s considered. For each pattern quality, 50 consistent quality masonry textures have been generated. Furthermore, additional 50 samples have been created with the generator developed by Vadalà et al. (Caprili et al., 2017), in which the unit dimensions have been taken consistently with the Normal quality masonry pattern described above, while no considerations on the QI-s have been considered. In total, 4 × 50 = 200 specimens have been simulated via a computer program which implements a micro limit analysis algorithm (Szabó et al., 2022; Gilbert et al., 2006) and the resulting horizontal load factors (λ) have been collected. One should note how the results are scale independent since mass proportional loading has been considered without the involvement of overload.

Fig. 29 represents the distribution of load factors of the generated

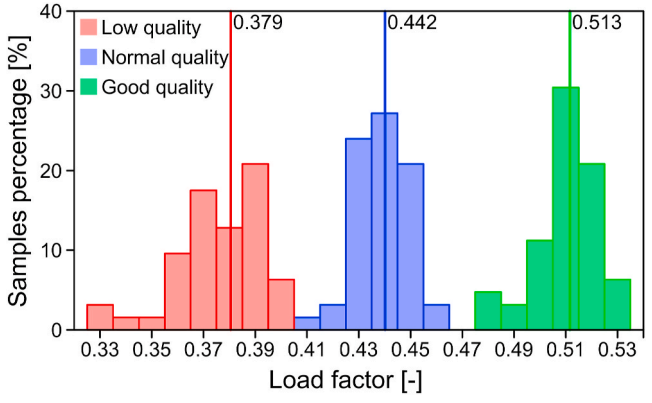

Fig. 29. Distribution of the simulated load factors corresponding to different masonry patterns quality.

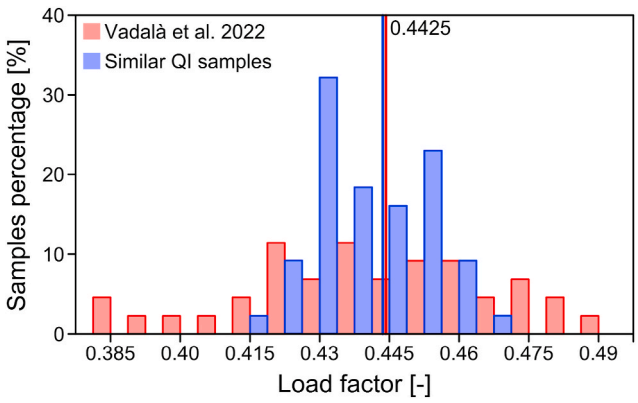

Fig. 30. Distribution of the simulated load factors. Comparison between the samples generated with similar QI-s and ones generated by Vadalà et al. (Vadalà et al., 2022) algorithm.

samples, considering the masonry pattern's quality. One can observe how the average values of the Normal and Good quality samples increase by a percentage equal to 14% and 26%, concerning the Low quality masonry patterns. Furthermore, Fig. 29 shows a reduction of the results scattering, with coefficients of variation passing from 4.48% for Low quality, to 2.43% and 2.13% for the Normal and Good quality masonries, respectively.

In Fig. 30, the results of the Normal quality masonry patterns (from Fig. 29) are compared with masonry patterns generated with the tool developed by Vadalà et al. (2022). Such a comparison underlines how, even though the mean values are approximately the same, their generator produced larger scattering in terms of load factor (Fig. 30). The coefficient of variation of the load factors is about double (4.73% vs 2.34%). The results underline how masonry specimens with similar QI-s are characterised by relatively uniform structural behaviour. It is worth remarking that generator algorithms, including the skillfulness of the masons and, consequently, QI-s, are correlated with the structural performance, resulting in the possibility of simulating several scenarios and making correlations between the simulation input parameters and the response measure.

Due to the significant effect on the structural behaviour, assessment of HMS should include the systematic treatment of QI-s to consider the effect of masonry patterns.

To this end, a general workflow is described in Fig. 31. The first stage involves the detection of the QI-s via NDT, which might be performed on one or multiple representative windows of the structure under investigation. Then, the quantitative assessment of the QI-s shed light on the proneness of the structure to fail in a specific mode. One should note how both numerical and experimental investigations must be performed within the scope to find a correlation between QI-s and predominant failure modes, e.g. monolithic behaviour, disaggregation, etc. The outcome of the former stage drives the identification of the most suitable computational approach for simulating the case of the study (Fortunato et al., 2017; Funari et al., 2020a, 2020b, 2021b, 2021c, 2022b; Cattari et al., 2021; Castellazzi et al., 2017; Degli Abbati et al., 2019; Pantò et al., 2017; Giresini et al., 2019). Afterwards, an extensively semi-probabilistic numerical campaign can be performed by generating several masonry samples consistent with the QI-s surveyed at the first step of the proposed workflow (Fig. 31). Other uncertainty sources, which are not detectable during the inspection, such as cross-section patterns, mechanical properties, loads and boundary conditions, might be introduced. A statistical analysis of the obtained RMs will allow identifying which parameters mostly affect the structural performance. Hence, additional NDT tests are recommended to refine the probabilistic assessment. One should note how the proposed workflow might also include other sources of uncertainty, i.e. material properties.

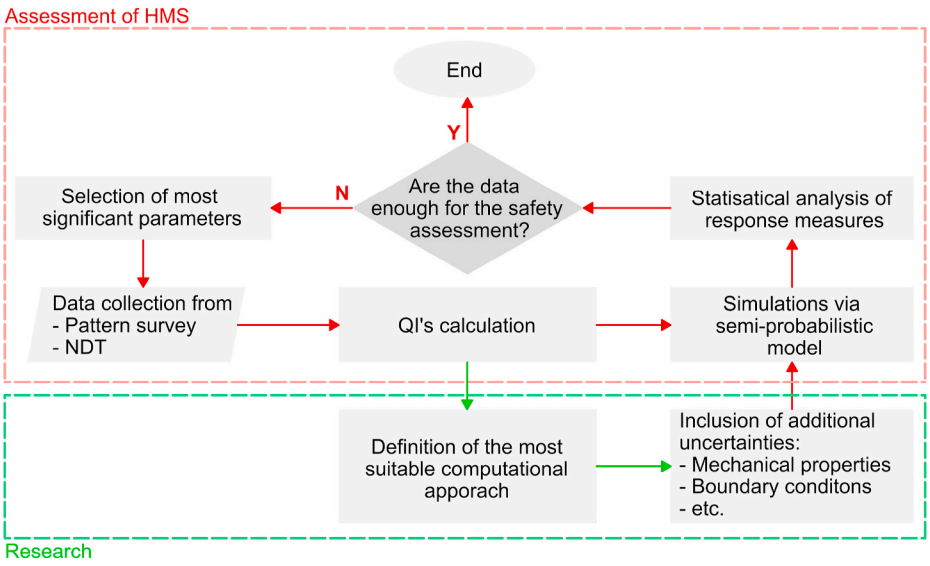

Fig. 31. Steps of the proposed framework to treat masonry patterns and additional uncertainties in the seismic assessment of HMS.

4. Final remarks

This paper presents a comprehensive literature review of masonry typologies and their characterisation through geometric measures, i.e. QI-s. The following points summarise the finding of this study.

- Ancient builders consciously tended towards universal good practices, following the so-called "rules of art", which provide an efficient measure for assessing the quality of masonry patterns of any type.
- The masonry pattern quality can be measaured with QI-s. These provide a quantitative characterisation of masonry patterns compared to the qualitative criteria in engineering and standard classifications.
- The quality of the masonry concurs with boundary and loading conditions to define the structural performance of HMS.
- QI-s are generally interdependent. Their coupled effect is usually neglected in the existing literature, bringing in erroneous evaluations of the masonry patterns' effect.
- QI-s treated singularly cannot adequately describe masonry structural behaviour. Consequently, a set of QI-s is needed to characterise masonry patterns properly.
- NDT allows the surveying of masonry patterns while minimising invasiveness. However, the cross-section survey is still challenging. Thus, the effect of morphology must be assessed following a probabilistic approach rather than a deterministic one.
- In conjunction with surveying, masonry pattern generator algorithms enable the systematic study of masonry pattern quality. Therefore, the importance of implementing proper digital tools to generate masonry specimens with consistent QI-s, has been underlined.
- Even after extensive surveying, the level of knowledge of an HMS is characterised by a level of uncertainty. Thus, probabilistic approaches should be developed, accounting for limited knowledge of the structure under investigation.
- Quantitative interdependence of QI-s will be investigated in future works by using multidimensional analysis tools such as Principal Component Analysis

Credit author statement

Simon Szabó: Conceptualisation. Methodology. Writing – original draft. Visualisation. Marco Francesco Funari: Methodology. Supervision. Writing – original draft. Paulo B. Lourenço: Funding acquisition. Supervision. Writing – review & editing.

Funding

This work was partly financed by FCT/MCTES through national funds (PIDDAC) under the R&D Unit ISISE under reference UIDB/04029/2020. This study has been partly funded by the STAND4-HERITAGE project that has received funding from the European Research Council (ERC) under the European Union's Horizon 2020 research and innovation program (Grant agreement No. 833123), as an Advanced Grant.

Declaration of competing interest

The authors declare that they have no known competing financial interests or personal relationships that could have appeared to influence the work reported in this paper.

Data availability

No data was used for the research described in the article.

References

Almeida, C., Guedes, J.M., Coelho, A.J., Arêde, D., 2014. Shear-Compressive experimental behaviour of one-leaf stone masonry walls in North of Portugal. In: Second European Conference on Earthquake Engineering. Istanbul. https://www.researchgate.net/publication/274719517. (Accessed 25 April 2022).

Almeida, C., Guedes, J.P., Arêde, A., Costa, A., 2016. Geometric indices to quantify textures irregularity of stone masonry walls. Construct. Build. Mater. 111, 199–208. https://doi.org/10.1016/j.conbuildmat.2016.02.038.

Angiolilli, M., Pathirage, M., Gregori, A., Cusatis, G., 2021. Lattice discrete particle model for the simulation of irregular stone masonry. J. Struct. Eng. 147, 04021123 https://doi.org/10.1061/(asce)st.1943-541x.0003093.

Arêde, A., Almeida, C., Costa, C., Costa, A., 2019. In-situ and lab tests for mechanical characterization of stone masonry historical structures. Construct. Build. Mater. 220, 503–515. https://doi.org/10.1016/J.CONBUILDMAT.2019.06.039.

B. Indian Standards, 1992. Construction of Stone Masonry - Code of Practice, vol. 1. Rubble Stone Masonry. IS 1597-1 (1992):

Baggio, C., Carocci, C., 2000. Valutazione della qualità meccanica delle murature. In: La Vulnerabilità Degli Edifici, Valutazione a Scala Nazionale Della Vulnerabilità Sismica Degli Edifici Ordinari, pp. 51–66.

Bernardi, A., 2000. La Vulnerabilità Degli Edifici: Valutazione a Scala Nazionale Della Vulnerabilità Sis-Mica Degli Edifici Ordinari. CNR-Gruppo Nazionale per la Difesa dai Terremoti, Rome.

Binda, L., 2001. State of the Art of Research on Historic Structures in Italy Historic Masonry Structures View Project Masonry Materials Testing View Project. https://www.researchgate.net/publication/237440027.

Binda, L., Saisi, A., 2009. Application of NDTs to the diagnosis of historic structures. In: NDTCE'09, Non-destructive Testing in Civil Engineering.
Binda, L., Fontana, A., Anti, L., 1991. Load transfer in multiple leaf walls. In: 9th Int Brick/Block Masonry Conf, pp. 1488–1497. Berlin, Germany.
Binda, L., Fontana, A., Mirabella, G., 1994. Mechanical behaviour and stress distribution in multiple-leaf stone walls. In: Proceedings of the 10th International Brick and Block Masonry Conference. Canada, Calgary, Alberta, pp. 51–60.
Binda, L., Modena, C., Baronial, G., Abbaneol, S., 1997. Repair andInvestigation techniques for stone masonry walls. Construct. Build. Mater. 11, 133–142.
Binda, L., Baronio, D., Penazzi, M., Tiraboschi, C., 1999. Caratterizzazione di Murature in Pietra in Zona Sismica Data-base Sulle Sezioni Murarie e Indagini sui Materiali.
Binda, L., Cardani, G., Saisi, A., 2005. A classification of structures and masonries for the adequate choice of repair. In: International RILEM Workshop on Repair Mortars for Historic Masonry.
Binda, L., Pina-Henriques, J., Anzani, A., Fontana, A., Lourenço, P.B., 2006. A contribution for the understanding of load-transfer mechanisms in multi-leaf masonry walls: testing and modelling. Eng. Struct. 28, 1132–1148. https://doi.org/10.1016/j.engstruct.2005.12.004.
Borri, A., Corradi, M., Castori, G., de Maria, A., 2015. A method for the analysis and classification of historic masonry. Bull. Earthq. Eng. 13, 2647–2665. https://doi.org/10.1007/s10518-015-9731-4.
Borri, A., Corradi, M., de Maria, A., 2020. The failure of masonry walls by disaggregation and the masonry quality index. Heritage 3, 1162–1198. https://doi.org/10.3390/heritage3040065.
Bosiljkov, V., Bokan-Bosiljkov, V., Strah, B., Velkavrh, J., Gostič, P., 2010. Review of Innovative Techniques Forthe Knowledge of Cultural Assets (Geometry, Technologies, Decay).
Bosiljkov, V., D'Ayala, D., Novelli, V., 2015. Evaluation of uncertainties in determining the seismic vulnerability of historic masonry buildings in Slovenia: use of macro-element and structural element modelling. Bull. Earthq. Eng. 13, 311–329. https://doi.org/10.1007/S10518-014-9652-7.
British Standards Institution, BS 5390:1976 Code of Practice for Stone Masonry, 1984.
Calderini, C., Cattari, S., Lagomarsino, S., 2010. The use of the diagonal compression test to identify the shear mechanical parameters of masonry. Construct. Build. Mater. 24, 677–685. https://doi.org/10.1016/J.CONBUILDMAT.2009.11.001.
Caliò, I., Pantò, B., 2005. A simplified model for the evaluation of the seismic behaviour of masonry buildings. https://doi.org/10.4203/ccp.81.195.
Caprili, S., Mangini, F., Paci, S., Salvatore, W., Bevilacqua, M.G., Karwacka, E., Squeglia, N., Barsotti, R., Bennati, S., Scarpelli, G., Iannelli, P., 2017. A knowledge-based approach for the structural assessment of cultural heritage, a case study: La Sapienza Palace in Pisa. Bull. Earthq. Eng. 15, 4851–4886. https://doi.org/10.1007/S10518-017-0158-Y.
Carbonara, G., 1996. Trattato di restauro arehitettonico. Utet, Torino.
Casapulla, C., Portioli, F., Maione, A., Landolfo, R., 2013. A macro-block model for in-plane loaded masonry walls with non-associative Coulomb friction. Meccanica 48, 2107–2126. https://doi.org/10.1007/s11012-013-9728-5.
Casapulla, C., Argiento, L.U., Maione, A., Speranza, E., 2021. Upgraded formulations for the onset of local mechanisms in multi-storey masonry buildings using limit analysis. Structures 31, 380–394. https://doi.org/10.1016/J.ISTRUC.2020.11.083.
Castellazzi, G., D'Altri, A.M., de Miranda, S., Ubertini, F., 2017. An innovative numerical modeling strategy for the structural analysis of historical monumental buildings. Eng. Struct. 132, 229–248. https://doi.org/10.1016/j.engstruct.2016.11.032.
Caterina, F., 2001. Carocci, Guidelines for the safety and preservation of historical centres in seismic areas. In: Historical Constructions. Guimarães, pp. 145–166.
Cattari, S., Camilletti, D., D'Altri, A.M., Lagomarsino, S., 2021. On the use of continuum Finite Element and Equivalent Frame models for the seismic assessment of masonry walls. J. Build. Eng. 43, 102519 https://doi.org/10.1016/J.JOBE.2021.102519.
Chen, S., Bagi, K., 2020. Crosswise tensile resistance of masonry patterns due to contact friction. Proc. Math. Phys. Eng. Sci. 476, 20200439 https://doi.org/10.1098/rspa.2020.0439.
Como, M., 2016. Springer Series in Solid and Structural Mechanics 5 Statics of Historic Masonry Constructions, second ed. http://www.springer.com/series/10616.
Corradi, M., Borri, A., Vignoli, A., 2003. Experimental study on the determination of strength of masonry walls. Construct. Build. Mater. 17, 325–337. https://doi.org/10.1016/S0950-0618(03)00007-2.
CSA Standard S304.1-94, 1994. Masonry Design for Buildings (Limit States Design). Canadian Standards, Association, Rexdale, Ontario, n.d.
Cusatis, G., Zdeně, Baž, P., Asce, F., Cedolin, L., Asce, M., 2003. Confinement-shear lattice model for concrete damage in tension and compression: II. Computation and validation. https://doi.org/10.1061/ASCE0733-93992003129:121449.
Davis, L., Rippmann, M., Pawlofsky, T., Block, P., 2012. Innovative funicular tile vaulting. Struct. Eng. 90, 46–56.
de Felice, G., 2005. Out-of-plane fragility of historic masonry walls. In: Conf. On Structural Analysis of Historical Constructions.
de Felice, G., 2011. Out-of-plane seismic capacity of masonry depending on wall section morphology. Int. J. Architect. Herit. 5, 466–482. https://doi.org/10.1080/15583058.2010.530339.
de Felice, G., Fugger, R., Gobbin, F., 2022a. Overturning of the façade in single-nave churches under seismic loading. Bull. Earthq. Eng. 20, 941–962. https://doi.org/10.1007/s10518-021-01243-5.
de Felice, G., Liberatore, D., de Santis, S., Gobbin, F., Roselli, I., Sangirardi, M., AlShawa, O., Sorrentino, L., 2022b. Seismic behaviour of rubble masonry: shake table test and numerical modelling. Earthq. Eng. Struct. Dynam. 51, 1245–1266. https://doi.org/10.1002/eqe.3613.
Degli Abbati, S., D'Altri, A.M., Ottonelli, D., Castellazzi, G., Cattari, S., de Miranda, S., Lagomarsino, S., 2019. Seismic assessment of interacting structural units in complex historic masonry constructions by nonlinear static analyses. Comput. Struct. 213, 51–71.
Deuss, M., Panozzo, D., Whiting, E., Liu, Y., Block, P., Sorkine-Hornung, O., Pauly, M., 2014. Assembling self-supporting structures. ACM Trans. Graph. 33 https://doi.org/10.1145/2661229.2661266.
Doglioni, F., Roberti, G.M., 2004. Valutazione speditiva della vulnerabilità sismica di murature in pietra: un caso di studio. In: XI Congresso Nazionale "L'ingegneria Sismica in Italia", pp. 25–29. Genova.
D'Ayala, D.F., Paganoni, S., 2011. Assessment and analysis of damage in L'Aquila historic city centre after 6th April 2009. Bull. Earthq. Eng. 9, 81–104. https://doi.org/10.1007/s10518-010-9224-4.
Elghazouli, A.Y., Bompa, D.v., Mourad, S.A., Elyamani, A., 2022a. Structural behaviour of clay brick lime mortar masonry walls under lateral cyclic loading in dry and wet conditions. Lecture Notes in Civil Engineering 164–174. https://doi.org/10.1007/978-3-030-90788-4_16/COVER, 209 LNCE.
Elghazouli, A.Y., Bompa, D.v., Mourad, S.A., Elyamani, A., 2022b. Seismic Performance of Heritage Clay Brick and Lime Mortar Masonry Structures, pp. 225–244. https://doi.org/10.1007/978-3-031-15104-0_14/COVER.
Ferreira Pinto, A.P., Sena da Fonseca, B., Vaz Silva, D., 2021. Mechanical characterization of historical rubble stone masonry and its correlation with the masonry quality assessment. Construct. Build. Mater. 281 https://doi.org/10.1016/J.CONBUILDMAT.2020.122168.
Fortunato, G., Funari, M.F., Lonetti, P., 2017. Survey and seismic vulnerability assessment of the baptistery of san giovanni in tumba (Italy). J. Cult. Herit. https://doi.org/10.1016/j.culher.2017.01.010.
Funari, M.F., Spadea, S., Lonetti, P., Fabbrocino, F., Luciano, R., 2020a. Visual programming for structural assessment of out-of-plane mechanisms in historic masonry structures. J. Build. Eng. 31, 101425 https://doi.org/10.1016/j.jobe.2020.101425.
Funari, M.F., Spadea, S., Ciantia, M., Lonetti, P., Greco, F., 2020b. Visual Programming for the Structural Assessment of Historic Masonry Structures. REHABEND.
Funari, M.F., Mehrotra, A., Lourenço, P.B., 2021a. A tool for the rapid seismic assessment of historic masonry structures based on limit analysis optimisation and rocking dynamics. Appl. Sci. 11, 942. https://doi.org/10.3390/app11030942.
Funari, M.F., Hajjat, A.E., Masciotta, M.G., Oliveira, D.v., Lourenço, P.B., 2021b. A parametric scan-to-FEM framework for the digital twin generation of historic masonry structures. Sustainability 13, 11088. https://doi.org/10.3390/SU131911088, 11088. 13 (2021).
Funari, M.F., Silva, L.C., Mousavian, E., Lourenço, P.B., 2021c. Real-time Structural Stability of Domes through Limit Analysis: Application to St. Peter's Dome, pp. 1–23. https://doi.org/10.1080/15583058.2021.1992539. Https://Doi.Org/10.1080/15583058.2021.1992539.
Funari, M.F., Pulatsu, B., Szabó, S., Lourenço, P.B., 2022a. A Solution for the Frictional Resistance in Macro-Block Limit Analysis of Non-periodic Masonry. STRUCTURES.
Funari, M.F., Silva, L.C., Savalle, N., Lourenço, P.B., 2022b. A concurrent micro/macro FE-model optimized with a limit analysis tool for the assessment of dry-joint masonry structures. Int. J. Multiscale Comput. Eng. https://doi.org/10.1615/IntJMultCompEng.2021040212 (in press).
Gilbert, M., Casapulla, C., Ahmed, H.M., 2006. Limit analysis of masonry block structures with non-associative frictional joints using linear programming. Comput. Struct. 84, 873–887. https://doi.org/10.1016/j.compstruc.2006.02.005.
Giresini, L., Pantò, B., Caddemi, S., Caliò, I., 2019. Out-of-plane seismic response of masonry façades using discrete macro-element and rigid block models. COMPDYN Proceedings 1, 702–717. https://doi.org/10.7712/120119.6950.19405.
Giuffrè, A., 1990. Letture Sulla Meccanica Delle Murature Storiche. Kappa, Rome.
Giuffré, A., 1996. A mechanical model for statics and dynamics of historical masonry buildings. In: Protection of the Architectural Heritage against Earthquakes. Springer, Vienna, pp. 71–152.
Giuffre, A., Pagnoni, T., Tocci, C., 1994. In-plane Seismic Behavior of Historic Masonry Walls, 10th International Brick and Block Masonry Conference.
GNDT/SNN, 2002. Manuale per la compilazione della scheda di 1° livello di rilevamento danno, pronto intervento e agibilità per edifici ordinari nell'emergenza post-sismica, Dipartimento Della Protezione Civile. EditriceAdel Grafica, Roma.
Gonen, S., Pulatsu, B., Soyoz, S., Erdogmus, E., 2021. Stochastic discontinuum analysis of unreinforced masonry walls: lateral capacity and performance assessments. Eng. Struct. 238 https://doi.org/10.1016/j.engstruct.2021.112175.
Guo, Y.T., Bompa, D.v., Elghazouli, A.Y., 2022. Nonlinear numerical assessments for the in-plane response of historic masonry walls. Eng. Struct. 268, 114734 https://doi.org/10.1016/J.ENGSTRUCT.2022.114734.
Howlader, M.K., Masia, M.J., Griffith, M.C., 2020. Numerical analysis and parametric study of unreinforced masonry walls with arch openings under lateral in-plane loading. Eng. Struct. 208 https://doi.org/10.1016/j.engstruct.2020.110337.
Ibrahim, Y., Nagy, B., Benedek, C., 2019. CNN-Based Watershed Marker Extraction for Brick Segmentation in Masonry Walls.
IMIT 2009, 2009. Ministry of Infrastructures and transportation. In: Istruzioni per l'applicazione delle nuove norme tecniche per le costruzioni di cui al Decreto Ministeriale 14 Gennaio 2008, vol. 47. G.U. S.O, p. 27. Circ. C.S.Ll.Pp. No. 617 of 2/2/2009.
International Charter for the Conservation and Restoration of Monuments and Sites, 1964. The Venice Charter).
Kržan, M., Gostič, S., Cattari, S., Bosiljkov, V., 2015. Acquiring reference parameters of masonry for the structural performance analysis of historical buildings. Bull. Earthq. Eng. 13, 203–236. https://doi.org/10.1007/s10518-014-9686-x.
Leslie, A., Mendes, N., Lourenço, P., 2017. The Effect of Morphology on the Structural Behaviour of Masonry Walls. Congreso de Métodos Numéricos En Ingeniería.

Lombardi, F., Lualdi, M., Garavaglia, E., 2021. Masonry texture reconstruction for building seismic assessment: practical evaluation and potentials of Ground Penetrating Radar methodology. Construct. Build. Mater. 299 https://doi.org/10.1016/j.conbuildmat.2021.124189.

Lourenço, P.B., Mendes, N., Costa, A.A., Campos-Costa, A., 2017. Methods and challenges on the out-of-plane assessment of existing masonry buildings. Int. J. Architect. Herit. 11, 1. https://doi.org/10.1080/15583058.2017.1237114.

Lulić, L., Ožić, K., Kišiček, T., Hafner, I., Stepinac, M., 2021. Post-earthquake damage assessment—case study of the educational building after the zagreb earthquake. Sustainability 13, 6353. https://doi.org/10.3390/SU13116353, 13 (2021) 6353.

Maheri, M.R., Najafgholipour, M.A., Rajabi, A.R., 2011. THE INFLUENCE OF MORTAR HEAD JOINTS ON THE IN-PLANE AND OUT-OF-PLANE SEISMIC STRENGTH OF BRICK MASONRY WALLS *.

Malomo, D., DeJong, M.J., Penna, A., 2021. Influence of bond pattern on the in-plane behavior of URM piers. Int. J. Architect. Herit. 15, 1492–1511. https://doi.org/10.1080/15583058.2019.1702738.

Mann, W., Müller, H., 1982. Failure of shear-stressed masonry - an enlarged theory, tests and application to shear walls. Proc. Br. Ceram. Soc. 223–235.

Marino, M., Neri, F., de Maria, A., Borri, A., 2014. Experimental Data of Friction Coefficient for Some Types of Masonry and its Correlation with an Index of Quality Masonry (IQM). Second European Conference on Earthquake Engineering.

Miyata, K., 1993. A method of generating stone wall patterns. Syst. Comput. Jpn. 24, 86–95.

Pantò, B., Giresini, L., Sassu, M., Caliò, I., 2017. Non-linear modeling of masonry churches through a discrete macro-element approach. Earthquake and Structures 12, 223–236. https://doi.org/10.12989/eas.2017.12.2.223.

Pulatsu, B., Gonen, S., Parisi, F., Erdogmus, E., Tuncay, K., Funari, M.F., Lourenço, P.B., 2022. Probabilistic approach to assess URM walls with openings using discrete rigid block analysis (D-RBA). J. Build. Eng. 61, 105269 https://doi.org/10.1016/j.jobe.2022.105269.

Quelhas Da Silva, B., Guedes, J.M., Quelhas, B., Cantini, L., Guedes, M., da Porto, F., Almeida, C., Quelhas, B., Porto, · F da, da Porto, F., Cantini, L., Guedes, J.M., Almeida, C., 2014. Characterization and reinforcement of stone masonry walls. In: Structural Rehabilitation of Old Buildings. https://doi.org/10.1007/978-3-642-39686-1_5.

Ramage H, M., Ochsendorf, J., Rich, P., Bellamy K, J., Block, P., 2021. Design and construction of the Mapungubwe national park interpretive center, South Africa. ATDF JOURNAL 7, 14–23.

Restrepo Vélez, L.F., Magenes, G., Griffith, M.C., 2014. Dry stone masonry walls in bending-Part I: static tests. Int. J. Architect. Herit. 8, 1–28. https://doi.org/10.1080/15583058.2012.663059.

Rezaie, A., Godio, M., Beyer, K., 2020. Experimental investigation of strength, stiffness and drift capacity of rubble stone masonry walls. Construct. Build. Mater. 251, 118972 https://doi.org/10.1016/J.CONBUILDMAT.2020.118972.

Rios, A.J., Pingaro, M., Reccia, E., Trovalusci, P., 2022. Statistical assessment of in-plane masonry panels using limit analysis with sliding mechanism. J. Eng. Mech. 148 https://doi.org/10.1061/(asce)em.1943-7889.0002061.

Rippmann, M., van Mele, T., Popescu, M., Augustynowicz, E., Méndez Echenagucia, T., Calvo Barentin, C.J., Frick, U., Block, P., 2016. The Armadillo Vault: computational design and digital fabrication of a freeform stone shell. Advances in Architectural Geometry 2016 344–363. https://doi.org/10.3218/3778-4_23.

Shaqfa, M., Beyer, K., 2022. A Virtual Microstructure Generator for 3D Stone Masonry Walls. European Journal of Mechanics - A/Solids, 104656. https://doi.org/10.1016/J.EUROMECHSOL.2022.104656.

Sithole, G., 2008. Detection of bricks in a masonry wall. Proc. Int. Arch. Photogramm. Remote Sens. Spatial Inf. Sci. 37, 567–572.

Stepinac, M., Gašparović, M., 2020. A review of emerging technologies for an assessment of safety and seismic vulnerability and damage detection of existing masonry structures. Appl. Sci. 10, 5060.

Stepinac, M., Kisicek, T., Renić, T., Hafner, I., Bedon, C., 2020. Methods for the assessment of critical properties in existing masonry structures under seismic loads—the ARES project. Appl. Sci. 10, 1576.

Swiss Society of Engineers and Architects SIA, 2003. SIA 266 Masonry. Zürich, Switzerland.

Szabó, S., Funari, M.F., Pulatsu, B., Lourenço, P.B., 2022. Lateral capacity of URM walls: a parametric study using macro and micro limit analysis predictions. Appl. Sci. 12, 10834. https://doi.org/10.3390/APP122110834, 12 (2022) 10834.

Taborda, R., Roten, D., 2015. Physics-based ground-motion simulation. In: Encyclopedia of Earthquake Engineering. Springer-Verlag, Berlin Heidelberg.

Taly, N., 2010. Design of Reinforced Masonry Structures, second ed.. McGraw-Hill Education, New York, 210AD.

The Charter of Krakow 2000 - Principles for Conservation and Restoration of Built Heritage, 2000.

Vaculik, J., Griffith, M.C., 2017. Probabilistic analysis of unreinforced brick masonry walls subjected to horizontal bending. J. Eng. Mech. 143, 04017056 https://doi.org/10.1061/(asce)em.1943-7889.0001266.

Vadalà, F., Cusmano, V., Funari, M.F., Caliò, I., Lourenço, P.B., 2022. On the use of a mesoscale masonry pattern representation in discrete macro-element approach. J. Build. Eng. 50.

Valero, E., Bosché, F., Forster, A., Wilson, L., Leslie, A., 2018. Evaluation of historic masonry. In: Heritage Building Information Modelling. Routledge, pp. 75–101. https://doi.org/10.4324/9781315628011-8.

Vanin, F., Zaganelli, D., Penna, A., Beyer, K., 2017. Estimates for the stiffness, strength and drift capacity of stone masonry walls based on 123 quasi-static cyclic tests reported in the literature. Bull. Earthq. Eng. 15, 5435–5479. https://doi.org/10.1007/s10518-017-0188-5.

Vasconcelos, G., Lourenço, P.B., 2009. In-plane experimental behavior of stone masonry walls under cyclic loading. J. Struct. Eng. 135, 1269–1277. https://doi.org/10.1061/(ASCE)ST.1943-541X.0000053.

Verstrynge, E., Lacidogna, G., Accornero, F., Tomor, A., 2021. A review on acoustic emission monitoring for damage detection in masonry structures. Construct. Build. Mater. 268 https://doi.org/10.1016/J.CONBUILDMAT.2020.121089.

Vlachakis, G., Vlachaki, E., Lourenço, P.B., 2020. Learning from failure: damage and failure of masonry structures, after the 2017 Lesvos earthquake (Greece). Eng. Fail. Anal. 117 https://doi.org/10.1016/j.engfailanal.2020.104803.

Vladimir, G., Haach, G., Vasconcelos, P.B., 2011. Lourenco, Parametrical Study of Masonry Walls Subjected to In-Plane Loading through Numerical Modeling. https://doi.org/10.1016/j.engstruct.2011.01.015.

Wigger, H., Budelmann, H., Fostasy, F., 2000. Methods of inspection and assessment of natural stone masonrybuildings: example of the Runneburg (Thüringen). In: Wittman, F.H., Verhoef, L.G.W. (Eds.), Brick Andbrickwork: Maintenance and Restrengthening of Materials and Structures. AEDIFICATIO Publisher, pp. 25–35123.

Zhang, S., Beyer, K., 2019. Numerical investigation of the role of masonry typology on shear strength. Eng. Struct. 192, 86–102. https://doi.org/10.1016/j.engstruct.2019.04.026.

Zhang, S., Taheri Mousavi, S.M., Richart, N., Molinari, J.F., Beyer, K., 2017. Micro-mechanical finite element modeling of diagonal compression test for historical stone masonry structure. Int. J. Solid Struct. 112, 122–132. https://doi.org/10.1016/J.IJSOLSTR.2017.02.014.

Zhang, S., Hofmann, M., Beyer, K., 2018. A 2D typology generator for historical masonry elements. Construct. Build. Mater. 184, 440–453. https://doi.org/10.1016/j.conbuildmat.2018.06.085.